

FedBaF: Federated Learning Aggregation Biased by a Foundation Model

Jong-Ik Park Srinivasa Pranav José M. F. Moura Carlee Joe-Wong

Electrical and Computer Engineering
Carnegie Mellon University

Abstract

Foundation models are now a major focus of leading technology organizations due to their ability to generalize across diverse tasks. Existing approaches for adapting foundation models to new applications often rely on Federated Learning (FL) and disclose the foundation model weights to clients when using it to initialize the global model. While these methods ensure client data privacy, they compromise model and information security. In this paper, we introduce Federated Learning Aggregation Biased by a Foundation Model (FedBaF), a novel method for dynamically integrating pre-trained foundation model weights during the FL aggregation phase. Unlike conventional methods, FedBaF preserves the confidentiality of the foundation model while still leveraging its power to train more accurate models, especially in non-IID and adversarial scenarios. Our comprehensive experiments use Pre-ResNet and foundation models like Vision Transformer to demonstrate that FedBaF not only matches, but often surpasses the test accuracy of traditional weight initialization methods by up to 11.4% in IID and up to 15.8% in non-IID settings. Additionally, FedBaF applied to a Transformer-based language model significantly reduced perplexity by up to 39.2%.

1 Introduction

Developing foundation models [1] has become a major focus for leading technology companies like OpenAI, Microsoft, and Amazon AWS. These deep learning models are often trained with vast amounts of high-quality data [2] and their ability to generalize across different tasks and domains has made them essential assets for industry, government, and academia. Foundation models have been applied to natural language processing (e.g., text generation, translation, summarization), image generation and recognition, healthcare diagnostics, finance predictive analytics, and customer service and virtual assistant tasks [3–7]. When a foundation model’s training data distribution

*Authors are partially supported by NSF Grant CNS-2409138, CNS-2106891, CNS-2312761, and CCF-2327905. Srinivasa Pranav is partially supported by NSF Graduate Research Fellowships (DGE-1745016, DGE-2140739) and an ARCS Fellowship.

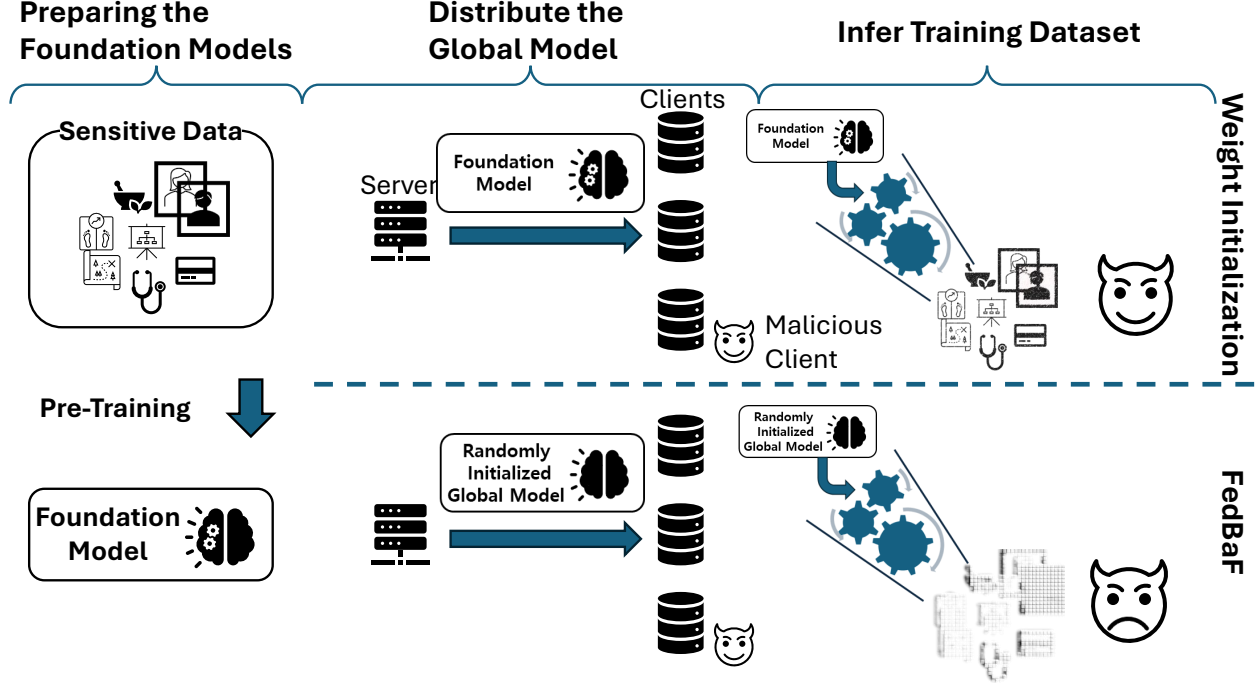


Figure 1: A visualization of a Model Inversion Attack. Since FedBaF does not initialize the global model with a pre-trained foundation model, it becomes difficult for malicious clients to reconstruct the pre-training data from the distributed global model.

overlaps with a new application, it provides a robust starting point for fine-tuning and customization. Instead of training a model from scratch, with limited data and compute, we can leverage pre-trained foundation models to enable faster training.

For many applications, data that could be used to customize or fine-tune foundation models is often distributed across multiple clients, such as a network of clinics or small companies spread across different jurisdictions. For example, fine-tuning a recommendation model to fit a small company’s product offering may require data from clients in various regions; and adapting a healthcare model for a network of clinics would involve distributed, confidential data sources. Therefore, effective generalization requires access to diverse data from multiple clients with similar objectives [8].

Federated Learning (FL) is a promising solution for fine-tuning these models without sharing client data: FL clients train models on diverse local data and a central FL server aggregates the client updates to build and refine a global model [9–14]. Using a foundation model to initialize the FL global model leads to effective customization that leverages diverse, distributed data without

directly accessing the client data [3,15]. However, *there are significant risks associated with sending a foundation model to clients, as required in traditional FL fine-tuning methods.*

First, disclosing a foundation model’s weights to FL clients poses a significant security risk. For example, malicious actors could carry out *membership inference attacks*, identifying whether specific data was part of the foundation model’s training dataset. Then, an attacker could disrupt the global model’s training by introducing updates that degrade performance on the identified data [16–18]. Similarly, for *model inversion attacks*, attackers reverse-engineer the model weights to infer sensitive training data (see Figure 1) [19–21]. Protecting foundation models, often trained on sensitive, proprietary data, is critical for safeguarding the training data and maintaining model integrity [22, 23].

Second, in competitive business contexts, disclosing foundation model weights to clients risks leaking strategic insights and proprietary information to adversaries [4, 24]. This undermines a company’s competitive advantage and substantial investments in data collection and training.

To address these challenges, we present Federated Learning Aggregation Biased by a Foundation Model (**FedBaF**). Rather than using a foundation model to initialize the global model, FedBaF is a novel method for server-side foundation model integration during the task-specific global model aggregation phase of each FL round (see Figure 2). Since the server uses the foundation model in the aggregation phase, FedBaF ensures that *the foundation model is not disclosed to clients*. FedBaF also gradually reduces the foundation model’s influence as training progresses, thereby improving personalization for the client pool’s data and matching or outperforming existing methods.

FedBaF is particularly beneficial for a FL operator who owns the foundation model and needs to maintain security and integrity while fine-tuning it with a new set of clients. For instance, large technology companies such as Microsoft and Amazon, develop their own foundation models and often act as FL operators for domain-specific tasks across various industries.

Our contributions:

1) To the best of our knowledge, we are the first to propose an **algorithm that integrates foundation models into FL without distributing the foundation model to clients**.

2) We provide **theoretical analysis of FedBaF’s effectiveness** that reveals how foundation models can promote convergence in non-IID (not independent and identically distributed) and

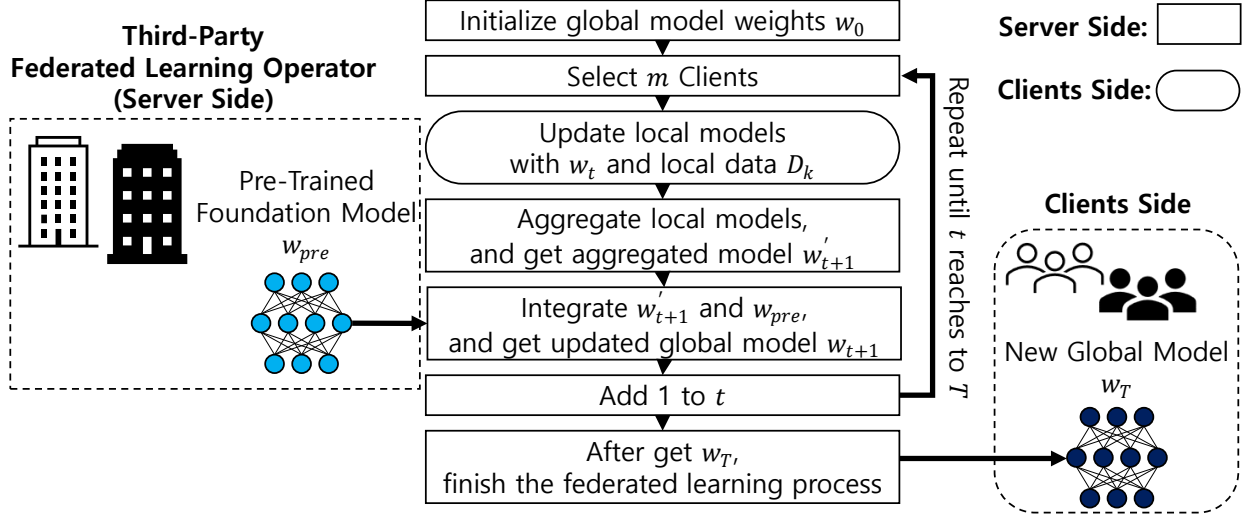


Figure 2: Visualization of FedBaF: in each FL round’s aggregation phase (after client updates), the server integrates a foundation model into the global model.

non-convex settings.

When client data distributions are biased or non-IID [25], e.g., different ratios or a lack of certain labels, clients optimize corresponding local objective functions and may send conflicting updates to the server that skew the global model [26]. In FedBaF, the foundation model continuously serves as a form of regularization and stabilizes the global model by reducing the influence of these conflicting updates during the aggregation phase [3, 7, 27, 28].

Furthermore, FedBaF uses a fixed foundation model as an anchor and continuously incorporates it throughout the FL training process. This adds a layer of protection from adversarial attacks beyond those introduced by disclosing foundation model weights – such as misclassification or backdoor attacks, where compromised clients feed malicious updates to the server [11, 22].

3) We conduct extensive empirical evaluation and show that **FedBaF matches or exceeds the training performance of traditional weight initialization methods** – with better test performance in 10 out of 14 cases. Our experiments use Pre-ResNet and more complex architectures like Vision Transformer and Transformer-based language models frequently used as foundation models [29, 30]. Compared to standard FedAvg [10] and FedProx [31], FedBaF achieves accuracy improvements of up to 10.8% in IID and up to 37.5% globally and 5.9% locally in non-IID settings. Simultaneously, FedBaF safeguards the foundation model. Similarly, applying FedBaF to a Transformer-based language model significantly reduced perplexity by up to 76.0%.

Under adversarial backdoor misclassification attacks, FedBaF demonstrates increased robustness by improving FedAvg and FedProx test performance by up to 19.4% in IID environments, up to 64.7% globally, and 7.2% locally in non-IID environments. Additionally, in 8 out of 12 cases, FedBaF was more robust than traditional weight initialization methods.

We outline related works in Sec. 2. We then detail our approach, FedBaF, in Sec. 3. In Sec. 4, we present theoretical analysis and, in Sec. 5, we provide extensive experimental evaluation. Finally, we conclude our research findings and discussion in Sec. 6.

2 Related Work

Traditionally, pre-trained models are used in FL to initialize the weights of the global FL model. The server distributes this model to local clients, and the clients update it with their local data. Such fine-tuning can significantly improve the FL model by integrating data from new clients, as supported by studies like FPS [3] and FedPCL [28].

Several works explore the use of foundation models in FL, particularly in scenarios with limited pre-training data [3]. This approach often involves using synthetic data [3, 32] for pre-training.

Federated Prototype-wise Contrastive Learning (FedPCL) is a significant development that aims to improve communication efficiency in FL by using class prototypes [28]. FedPCL enhances personalized learning by having clients share class-specific information more effectively. It fuses representations from multiple pre-trained models (backbones) at each client, with prototypes serving as the primary medium of information exchange. The strategy reduces communication overhead and enables customizing local models without extensive weight synchronization.

The related works discussed in this section achieve good performance, but they do not consider the significant **security vulnerabilities** that result from sharing a foundation model with local clients, which compromise data privacy and the integrity of the global model. Malicious clients with access to foundation models can exploit them through: Model Inversion Attacks, recovering original training data or sensitive attributes from the model’s outputs [19–21]; Membership Inference Attacks, analyzing model predictions to determine whether specific data records were used in training [16–18]. These attacks compromise the security of the FL system, necessitating the

development of more secure methods for leveraging pre-trained foundation models in FL settings.

FedBaF addresses these security challenges by not sharing the foundation model with clients during the weight initialization stage. Instead, it dynamically integrates the foundation model’s pre-trained weights during the aggregation phase of each training round.

3 FedBaF Methodology

In this section, we introduce FedBaF, whose approach is illustrated in Figure 2. During the aggregation phases of the FL training process, our FedBaF method repeatedly leverages pre-trained foundation model weights. For example, the pre-trained weights corresponding to feature extraction layers provide valuable representation mappings that guide the new model’s feature extractor during training. This approach can also extend to other layers if the foundation and FL models share the same architecture. When the new FL model has different neural network layers from the foundation model, i.e, the classifier layers, these different layers’ parameters are randomly initialized and then trained using data from the client pool, as in standard FL.

Algorithm 1 Federated Learning Aggregation Biased by a Foundation Model (FedBaF).

```

1: Initialize global model weights  $\mathbf{w}_0$ 
2: for each round  $t = 0, 1, 2, \dots, T$  do
3:    $m \leftarrow \max(C \cdot K, 1)$ 
4:    $S_t \leftarrow$  (random set of  $m$  clients)
5:   for each client  $k \in S_t$  in parallel do
6:      $\mathbf{w}_{t+1}^k \leftarrow \text{ClientUpdate}(\mathbf{w}_t, D_k)$ 
7:   end for
8:    $\mathbf{w}'_{t+1} \leftarrow \sum_{k \in S_t} \frac{n_k}{\sum_{k \in S_t} n_k} \mathbf{w}_{t+1}^k$ 
9:    $\tau_t \leftarrow \frac{\left\| \frac{\mathbf{w}'_{t+1}}{\|\mathbf{w}'_{t+1}\|} - \frac{\mathbf{w}_t}{\|\mathbf{w}_t\|} \right\|}{\sqrt{t+1}}$ 
10:   $\alpha_t \leftarrow \frac{\psi}{\tau_0} \text{U}(1, 2)$ 
11:   $\mathbf{w}_{t+1} \leftarrow \frac{1}{1+\alpha_t \tau_t} (\mathbf{w}'_{t+1} + \alpha_t \tau_t (\mathbf{w}_{pre} \setminus \mathbf{w}_t))$ 
12: end for
13: ClientUpdate( $\mathbf{w}, D$ )
14:   Initialize local model weights with  $\mathbf{w}$ 
15:   Update local model weights using local data  $D$ 
16: return updated model weights

```

Algorithm 1 describes how FedBaF fits into the traditional FL framework by incorporating foundation model weights during aggregation, as illustrated in *Lines 9-11* [10]. FedBaF is versatile

and can be embedded into many existing FL algorithms, e.g., SCAFFOLD [33], FedProx [31], or other FL strategies, by modifying their aggregation methods (*Lines 8-11*) and using their existing **ClientUpdate**(\mathbf{w}, D) logic for clients’ local training in *Line 13*.

Modifying FL aggregation. FedBaF’s aggregation process in each training round begins with the same step as FedAvg’s or many other FL algorithms’ aggregation, by computing a weighted sum of the updated model parameters from each client (*Line 8*). After this aggregation, in *Line 11* FedBaF incorporates the pre-trained model weights (\mathbf{w}_{pre}) into the global FL model, controlled by the factor τ_t defined in *Line 9*. Here, $(\mathbf{w}_{pre} \setminus \mathbf{w}_t)$ refers to *the subset of layers from the foundation model* (\mathbf{w}_{pre}) that have the same architecture as the corresponding layers in the global FL model (\mathbf{w}_t), ensuring that only compatible layers are used during aggregation.

Designing τ_t . Our careful design of τ_t uses the $L2$ norm of the difference between consecutive normalized weights of \mathbf{w}'_{t+1} and \mathbf{w}_t , divided by $\sqrt{t+1}$. This change in the model’s weights between rounds reflects how much the global model adapts to new client updates. The normalization prevents τ_t from becoming too large. The factor $\sqrt{t+1}$ ensures that, as training progresses, the influence of \mathbf{w}_{pre} gradually diminishes, but not too quickly, and \mathbf{w}_{t+1} approaches the improving averaged weights \mathbf{w}'_{t+1} . This strategy is critical to keeping the global model flexible and effective, especially when client data differs from the data used to train the foundation model [33].

Depending on the network architectures (e.g., the number of weights or scale of the initialized weights), the scale of τ_t can vary. In non-IID situations and during adversarial attacks, the factor τ_t becomes significant. In particular, a large τ can indicate the presence of non-IID data or an attack, as such scenarios often result in large differences in consecutive weight updates. To keep τ_t within a suitable range, we introduce the parameter α_t in *Line 10*, which depends on τ_0 and the hyper-parameter ψ . We empirically find that setting α_t such that $\alpha_t\tau_0$ is less than 2 in the initial round ($t = 0$) prevents excessively large values that could overly bias the global model towards the foundation model. A lower bound of 1 for $\alpha_t\tau_0$ also ensures that the minimum impact of the foundation model is significant for small t . We thus ensure the influence of the foundation model in the critical initial training stages, while still allowing the global model to adapt as training progresses.

Designing α_t . Sampling α_t from the uniform distribution $\frac{\psi}{\tau_0}\mathcal{U}(1, 2)$ for every round makes it

difficult for clients to reverse-engineer the foundation model, thus meeting FedBaF’s model security guarantees. To see this, *Line 11* can be rearranged for \mathbf{w}_{pre} as

$$\mathbf{w}_{pre} = \frac{(1 + \alpha_t \tau_t) \mathbf{w}_{t+1} - \mathbf{w}'_{t+1}}{\alpha_t \tau_t}.$$

In the worst-case scenario, where all local clients are malicious and collaborating to extract the foundation model’s weights, they can access τ_t , \mathbf{w}_{t+1} , and \mathbf{w}'_{t+1} . However, because α_t is randomly chosen in each round t and known only to the server, the foundation model’s weights cannot be extracted. If α were static, even if the server did not disclose it, malicious clients could determine this constant value by solving the residual equations from two successive rounds,

$$\frac{(1 + \alpha \tau_t) \mathbf{w}_{t+1} - \mathbf{w}'_{t+1}}{\alpha \tau_t} = \frac{(1 + \alpha \tau_{t+1}) \mathbf{w}_{t+2} - \mathbf{w}'_{t+2}}{\alpha \tau_{t+1}}.$$

This would eventually reveal the foundation model’s weights. *More details, along with empirical analysis on the role of α_t and the security advantages of FedBaF are provided in Appendix G.*

We formally examine this idea in the next section.

4 Theoretical Analysis of FedBaF

In this section, we focus on deriving performance guarantees for FedBaF, focusing on its convergence properties. Sec. 4.1 examines the general convergence behavior of FedBaF, while Sec. 4.2 shows specifically on how FedBaF manages convergence in the presence of diverse, non-IID local client data distributions.

The following notation, problem setup, and assumptions are used throughout our analysis. Given m clients, let the k th device’s training data be drawn from \mathcal{D}_k . The FL problem can be formulated as the following global objective,

$$\min_{\mathbf{w}} \frac{1}{\sum_{k=1}^m n_k} \sum_{k=1}^m n_k f_{\mathcal{D}_k}(\mathbf{w}), \quad (1)$$

where \mathbf{w} are model (usually, deep neural network) weights and the $f_{\mathcal{D}_k}$ are L -smooth local objective

functions. The convergence analysis presented in this section also makes the following standard assumptions made by [33] and detailed in Appendix E. Each client locally optimizes \mathbf{w} using stochastic gradient descent, where the stochastic gradients are (i) unbiased and (ii) have bounded variance. We also assume (iii) bounded gradient dissimilarity: the norm of the difference between the gradient of the global objective and the gradients computed using different local objective functions is bounded.

4.1 General Convergence Analysis

Proposition 1. *Let \mathbf{w}^* be a (bounded) local minimum of the global objective function in (1). Consider an FL algorithm that converges to \mathbf{w}^* and let \mathbf{w}'_t be its global model in each training round t . Suppose we run the same algorithm but using FedBaF for the aggregation, and let \mathbf{w}_t be the FedBaF global model at round t . Let α_t satisfy*

$$\alpha_t < \frac{2\|\mathbf{w}'_{t+1} - \mathbf{w}^*\|^2}{(\|\mathbf{w}_{pre} - \mathbf{w}^*\|^2 - \|\mathbf{w}'_{t+1} - \mathbf{w}^*\|^2)\tau_t} \quad (2)$$

for all t where $\|\mathbf{w}'_{t+1} - \mathbf{w}^\|^2 < \|\mathbf{w}_{pre} - \mathbf{w}^*\|^2$. Then $\forall t \|\mathbf{w}_t - \mathbf{w}^*\| < \|\mathbf{w}'_t - \mathbf{w}^*\|$.*

This means that, at any given round t , FedBaF's model weights are closer to \mathbf{w}^ .*

Using the same restrictions on local and global learning rates placed by the FedAvg convergence analysis in [33], the aforementioned bounded gradient variance, bounded gradient dissimilarity, and L-smoothness assumptions ensure that our method converges to \mathbf{w}^* faster than FedAvg. Similar convergence rate arguments for other FL methods with appropriately modified aggregation can be shown, as discussed in Sec. 3.

4.2 Effectiveness of FedBaF with Diverse Client Data

This section shows the impact of integrating a foundation model close to the optimal weights on the learning process and convergence behavior in non-IID environments.

In round t , client k uses multiple SGD steps to update the global model \mathbf{w}_t and obtains the local model \mathbf{w}_t^k . Letting S_t represent the randomly selected set of active clients at time t , we define

δ_t as the maximum deviation of the client models from \mathbf{w}^* :

$$\delta_t := \max_{k \in S_t} \|\mathbf{w}_t^k - \mathbf{w}^*\|.$$

Aggregating the updated models from clients according to Alg. 1 *Lines 8-10* forms the global model \mathbf{w}'_t , and then,

$$\delta_t \geq \|\mathbf{w}'_t - \mathbf{w}^*\|.$$

Assumption: Foundation Model Proximity. The foundation model’s pre-trained weights, \mathbf{w}_{pre} , are close to the optimal weights \mathbf{w}^* , i.e., $\|\mathbf{w}_{\text{pre}} - \mathbf{w}^*\| \leq \gamma$ for a small $\gamma > 0$. Furthermore, we assume that $\gamma \leq \delta_t$ for earlier rounds (small t which makes $\tau_t \gg 0$), i.e., the foundation model is closer to the optimal model than clients’ local weights.

These are reasonable assumptions in practice since selecting a foundation model with a large γ would correspond to selecting an unsuitable foundation model that hampers the training process.

Proposition 2. *Let \mathbf{w}^* be a (bounded) local minimum of the global objective function in (1). Consider an FL algorithm that converges to \mathbf{w}^* and let \mathbf{w}'_t be its global model. Consider FedBaF based on the same FL algorithm (with appropriately modified client updates and Lines 8-10 in Alg. 1) and let \mathbf{w}_t be the FedBaF global model. FedBaF’s global model error has an upper bound of $\|\mathbf{w}_t - \mathbf{w}^*\| \leq \frac{\delta_t + \alpha_t \tau_t \gamma}{1 + \alpha_t \tau_t} < \delta_t$.*

Similar to (29) in Sec. 4.1, we bounded the distance between the FedBaF global model \mathbf{w}_t and \mathbf{w}^* in terms of δ_t . Prop. 2 shows that the integration of the foundation model not only helps in stabilizing the learning process but also accelerates the convergence rate. The foundation model acts as a stabilizing factor and reduces the impact of this variance on the global model’s convergence. This is particularly significant in the early stages of learning with non-IID data, when local models’ weights are more prone to diverge from each other.

5 Experimental Evaluations

In this section, we conduct a detailed evaluation of FedBaF’s performance on both local and global test datasets, comparing its performance to the **no foundation model** cases and **weight initial-**

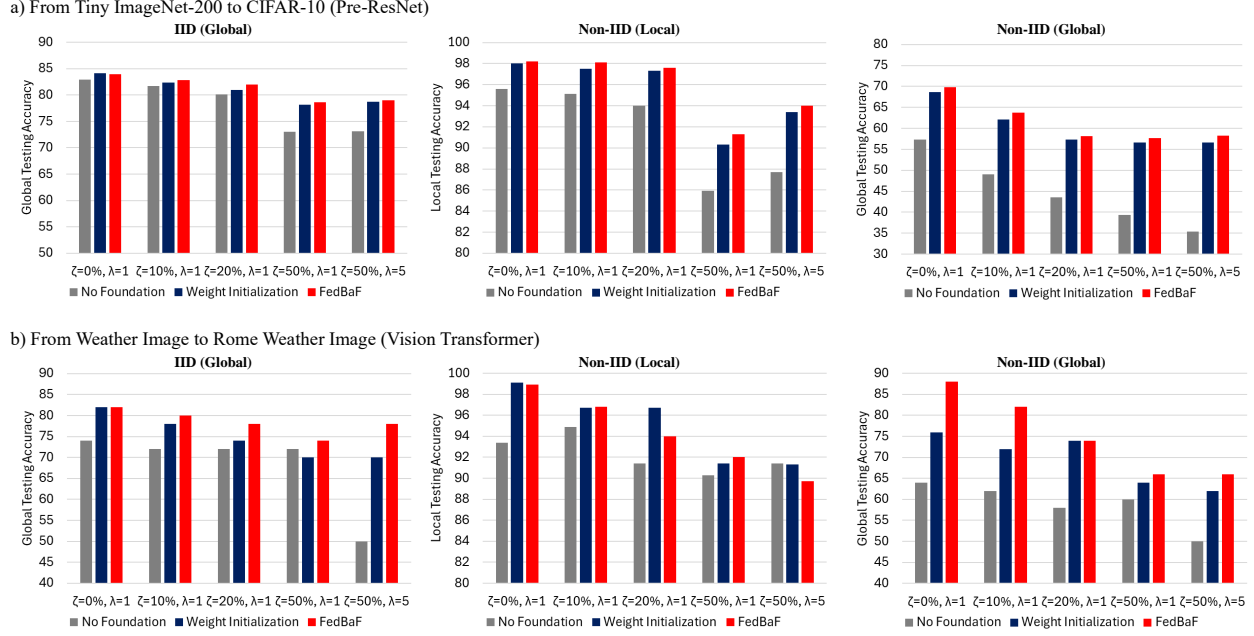


Figure 3: FedBaF maintains higher test accuracy when used with **FedAvg** with different proportions of malicious clients, ζ (0%, 10%, 20%, 50%), and attack intensity, λ (1, 5), executing misclassification attacks, under IID and non-IID settings. Three different foundation models, trained with different datasets, are used for three tasks. Red, blue, and gray bars respectively represent FedBaF, weight initialization, and no foundation model cases.

ization algorithms for training FL models.

- **No foundation model:** The global FL model is trained from scratch without weight initialization or FedBaF (i.e., no use of foundation models).
- **Weight initialization:** The global model’s initial weights are set to equal the foundation model’s weights, and the FL training then proceeds as usual.

We aim to **1)** illustrate that FedBaF offers security advantages over weight initialization while attaining equivalent performance. Furthermore, by verifying how τ_t in line 9 of Algorithm 1 converges to 0, we also **2)** establish FedBaF’s ability to effectively adapt the influence of the foundation model.

More detailed testing results are provided in Appendix C, including the **1)** computational efficiency of FedBaF and **2)** additional evaluations using foundation models of varying quality trained on different amounts of data and real-world foundation model weights that are officially available online.

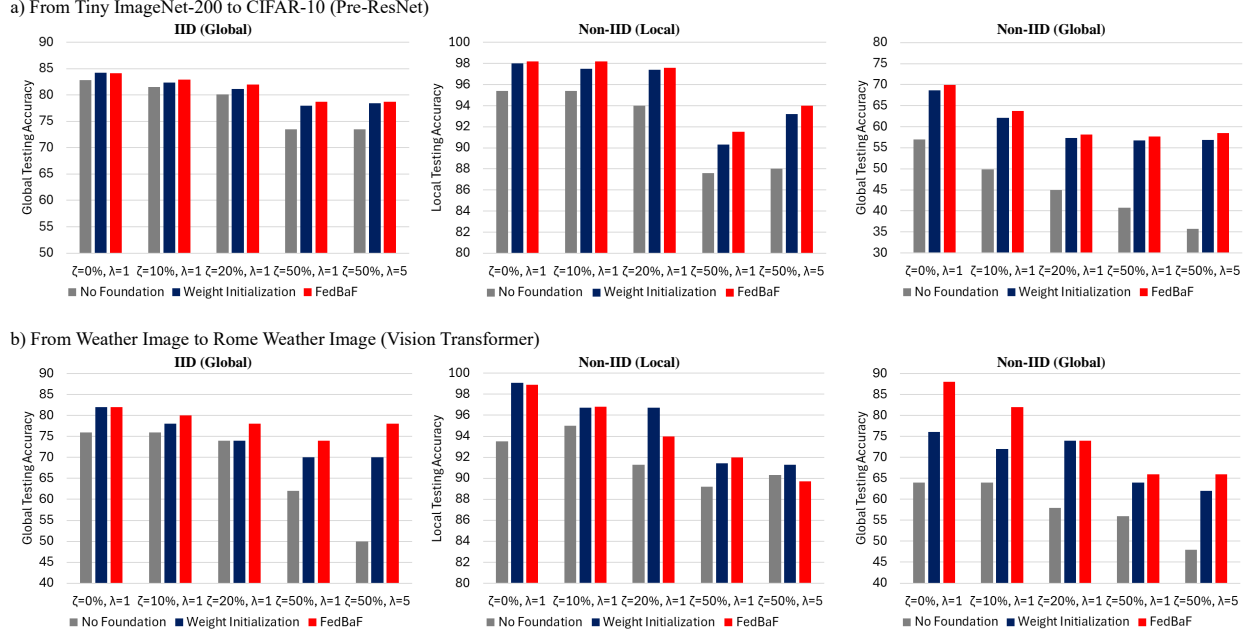


Figure 4: FedBaF maintains higher test accuracy than both baselines when used with **FedProx** with different proportions of malicious clients, attack intensity, and IID as well as non-IID settings. All other settings are identical to those in Figure 3.

5.1 Experimental Setup

Our experiments with popular image classification tasks encompass experiments using the CIFAR-10 and Rome Weather Image [34] datasets. We use Pre-ResNet and Vision Transformer [35] architectures as Vision Transformers are popular foundation model architectures known for achieving remarkable performance [36] for ImageNet challenges [35]. We train the foundation models on the Tiny ImageNet-200 and Weather Image [37] datasets. Our evaluations consider both IID and non-IID settings (see Appendix A) [38, 39]. To demonstrate FedBaF’s generalizability to other tasks, we also evaluate it on a next-word prediction task using a Transformer language model pre-trained on the WikiText-2 dataset and tested on the Penn Treebank dataset.

Attack setup. To assess security robustness of FedBaF, we randomly shuffle local data labels for a subset of clients, treating them as backdoor attackers aiming to induce misclassification. We also increase the attack intensity by varying the number of local epochs for malicious clients. For image classification tasks (Pre-ResNet and Vision Transformer), we increase the local epochs by a factor $\lambda > 1$, which introduces more bias from the initial global model and strengthens the attack’s impact. For the language task (Transformer), we decrease the local epochs by a factor $1/\lambda < 1$ to

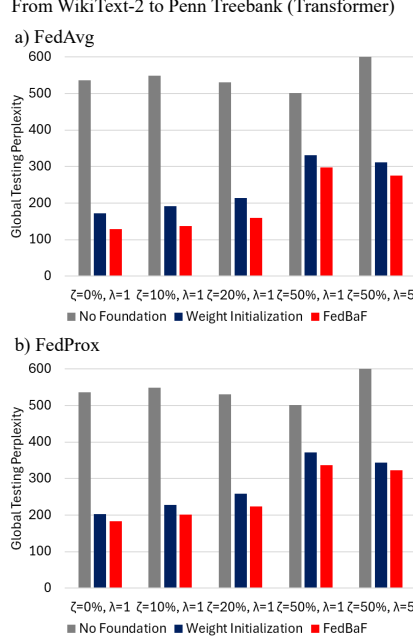


Figure 5: FedBaF maintains lower test perplexity when used with **FedAvg** and **FedProx** with different proportions of malicious clients and attack intensities. **Note: lower perplexity is better**

prevent convergence to a small loss, ensuring the calculated perplexity remains high regardless of misclassification, thereby intensifying the attack. We vary the proportion of attacking clients, ζ , and evaluate algorithm resiliency when 0%, 10%, 20%, and 50% of the client base are attackers.

Evaluation metrics. To evaluate testing performance, we calculate the *global testing accuracy* using a global test dataset after the aggregation phase of an FL round. In non-IID settings, we also use local test datasets that are extracted from the global test dataset and reflect the class distribution of the local clients. After local training and prior to aggregation, we test the local models to determine an *average local testing accuracy*. For the Transformer model, we use *global perplexity* to assess the performance of the global language model. Perplexity is **inversely** related to how well a probability model predicts a sample.

Details of other deep neural network architectures employed in our experiments and additional training specifics are provided in Tables 2 and 1 in Appendix A.

5.2 Experimental Results

Figures 3, 4, and 5 display the extensive test accuracy/perplexity evaluation results for FedBaF and our two baselines (*no foundation model* and *weight initialization*). We evaluate these three methods using both FedAvg and FedProx [31] as the base FL training algorithms. We incorporate FedBaF into FedProx by modifying *Line 8* and the ClientUpdate routine in Algorithm 1, including both IID and non-IID settings, with one non-adversarial scenario and four adversarial scenarios. We use FedProx’s usual aggregation equation $\mathbf{w}'_{t+1} \leftarrow \sum_{k \in S_t} \frac{n_k}{\sum_{k \in S_t} n_k} \mathbf{w}_{t+1}^k - \mu(\mathbf{w}_{t+1}^k - \mathbf{w}_t)$. Here, μ represents the regularization term that controls the trade-off between the local and global objectives. FedBaF then incorporates the foundation model weights as in *Lines 9-11* of Algorithm 1.

5.2.1 Testing Performance Enhancements

In non-adversarial scenarios, FedBaF showcased superior testing performance compared to the no foundation model and weight initialization methods across both IID and non-IID configurations.

Figures 3 and 4 respectively show the test accuracies of all three methods using FedAvg and FedProx for both Pre-ResNet and the Vision Transformer. In comparison to Pre-ResNet trained with no foundation model, FedBaF improved the global model’s accuracy by 1.3% for FedAvg and 1.6% for FedProx in IID scenarios, and by 21.8% for FedAvg and 22.6% for FedProx in non-IID scenarios. For the Vision Transformer, global performance improvements from FedBaF relative to no foundation model by 10.8% for FedAvg and 0.0% for FedProx in IID settings and 37.5% for FedAvg and 15.8% for FedProx in non-IID settings. We thus observe that **both FedAvg and FedProx benefit from FedBaF’s inclusion of the foundation model**, with particular benefits in the more challenging scenario with non-IID client data. Intuitively, non-IID data tends to slow FL convergence, which is mitigated by incorporating the foundation model.

The weight initialization method, which also incorporates a foundation model but does not keep it private, exhibits similar performance gains as FedBaF compared to training without a foundation model. For example, on Pre-ResNet weight initialization exhibited global performance gains of 19.7% for FedAvg and 20.4% for FedProx in non-IID scenarios, while on Vision Transformers it achieves gains of 18.8% for both FedAvg and FedProx in non-IID scenarios.

In the next-word prediction task using a Transformer, FedBaF significantly outperformed training with no foundation model, reducing perplexity by 76.0% with FedAvg, whereas weight initialization yielded a 67.8% decrease relative to training without a foundation model with FedAvg. Collectively, these findings indicate **negligible differences between the test accuracies attained by FedBaF and those achieved with weight initialization**, despite the fact that unlike weight initialization, FedBaF does not reveal the foundation model weights to FL clients. Moreover, FedBaF showed better testing performance than the weight initialization or no foundation model methods in 10 out of the 14 experiment settings.

5.2.2 Robustness to Attacks

FedBaF remains effective in maintaining robustness against misclassification attacks, showing a more modest performance decline than both baseline methods.

We next evaluate the robustness of FedBaF and our two baselines to adversarial clients. As the proportion of attacking clients (ζ in Figures 3, 4, and 5) increases, test accuracy declines in all cases, as we would intuitively expect since even FedBaF is not designed to perfectly defend against these attacks, which become more effective as more clients act as attackers.

The test accuracy for the no foundation model method especially drops significantly when 50% of the clients are attackers and the attack intensity $\lambda = 5$. For Pre-ResNet under such attacks, there is a global performance decrease compared to the case with no attackers of 11.8% for FedAvg and 11.2% for FedProx in IID scenarios and 38.2% for FedAvg and 37.4% for FedProx in non-IID scenarios. For Vision Transformer, these accuracy drops are 32.4% for FedAvg and 34.2% for FedProx in IID and 21.9% for FedAvg and 25.0% for FedProx in non-IID scenarios. Thus, **the no foundation model training method is vulnerable to attacks in both IID and non-IID settings**, as we would expect since it has no built-in defenses.

In contrast, **FedBaF experiences a much more modest performance decline under attack**, demonstrating its robustness. For Pre-ResNet, FedBaF’s global performance decreases by 6.0% for FedAvg and 6.4% for FedProx in IID settings and by 16.5% for FedAvg and 16.3% for FedProx in non-IID settings, where the decrease is again measured for the most intense attack ($\zeta = 50\%$, $\lambda = 5$ relative to no attack. These accuracy drops are *less than half* of those experienced by

the no foundation model method. For Vision Transformer, FedBaF’s global performance decreases by only 4.9% for FedAvg and FedProx in IID settings and by 25% for both FedAvg and FedProx in non-IID settings.

We finally see from the results for the weight initialization method that naïvely incorporating the foundation model still confers some robustness to attacks, though weight initialization reveals the foundation model weights to clients. Weight initialization shows a performance decrease of 6.4% for FedAvg and 6.9% for FedProx in IID settings and by 17.5% for FedAvg and 17.2% for FedProx in non-IID settings globally for Pre-ResNet. For Vision Transformer, the decreases are 14.6% for both FedAvg and FedProx in IID settings and by 18.4% for both FedAvg and FedProx in non-IID settings globally.

These findings demonstrate that, similar to weight initialization, **FedBaF offers considerable attack robustness** compared to training with no foundation model. In 8 out of 12 cases, FedBaF shows the minimum decrease in performance across all three methods, indicating its superior effectiveness in maintaining robustness under adversarial conditions.

6 Conclusion

This paper introduced Federated Learning Aggregation Biased by a Foundation Model (FedBaF). FedBaF enhances adaptability and security in dynamic FL scenarios without sharing the foundation model with clients. This is crucial in environments with ever-changing data and non-IID scenarios, where foundation models are used across several domains as seed models. Our findings show that FedBaF increases resilience against adversarial attacks while matching or outperforming traditional weight initialization performance in both IID and non-IID settings.

References

- [1] W. Zhuang, C. Chen, and L. Lyu, “When foundation model meets federated learning: Motivations, challenges, and future directions,” 2024.
- [2] R. Bommasani, D. A. Hudson, E. Adeli, R. Altman, S. Arora, S. von Arx, M. S. Bernstein, J. Bohg, A. Bosselut, E. Brunskill, *et al.*, “On the opportunities and risks of foundation models,” *arXiv preprint arXiv:2108.07258*, 2021.
- [3] H.-Y. Chen, C.-H. Tu, Z. Li, H. W. Shen, and W.-L. Chao, “On the importance and applicability of pre-training for federated learning,” in *The Eleventh International Conference on Learning Representations*, 2022.
- [4] X. Han, Z. Zhang, N. Ding, Y. Gu, X. Liu, Y. Huo, J. Qiu, Y. Yao, A. Zhang, L. Zhang, *et al.*, “Pre-trained models: Past, present and future,” *AI Open*, vol. 2, pp. 225–250, 2021.
- [5] M. Duan, D. Liu, X. Ji, Y. Wu, L. Liang, X. Chen, Y. Tan, and A. Ren, “Flexible clustered federated learning for client-level data distribution shift,” *IEEE Transactions on Parallel and Distributed Systems*, vol. 33, no. 11, pp. 2661–2674, 2021.
- [6] M. Joshi, A. Pal, and M. Sankarasubbu, “Federated learning for healthcare domain - pipeline, applications and challenges,” *ACM Trans. Comput. Healthcare*, vol. 3, nov 2022.
- [7] J. Yosinski, J. Clune, Y. Bengio, and H. Lipson, “How transferable are features in deep neural networks?,” *Advances in Neural Information Processing Systems*, vol. 27, 2014.
- [8] S. Pranav and J. M. Moura, “Peer-to-peer deep learning for beyond-5g iot,” *arXiv preprint arXiv:2310.18861*, 2023.
- [9] Q. Li, Z. Wen, Z. Wu, S. Hu, N. Wang, Y. Li, X. Liu, and B. He, “A survey on federated learning systems: Vision, hype and reality for data privacy and protection,” *IEEE Transactions on Knowledge and Data Engineering*, 2021.
- [10] B. McMahan, E. Moore, D. Ramage, S. Hampson, and B. A. y Arcas, “Communication-efficient

- learning of deep networks from decentralized data,” in *Artificial Intelligence and Statistics*, pp. 1273–1282, PMLR, 2017.
- [11] L. Lyu, H. Yu, J. Zhao, and Q. Yang, *Threats to Federated Learning*, pp. 3–16. Cham: Springer International Publishing, 2020.
 - [12] D. C. Nguyen, M. Ding, P. N. Pathirana, A. Seneviratne, J. Li, and H. V. Poor, “Federated learning for internet of things: A comprehensive survey,” *IEEE Communications Surveys & Tutorials*, vol. 23, no. 3, pp. 1622–1658, 2021.
 - [13] M. Siew, H. Zhang, J.-I. Park, Y. Liu, Y. Ruan, L. Su, S. Ioannidis, E. Yeh, and C. Joe-Wong, “Fair concurrent training of multiple models in federated learning,” *arXiv preprint arXiv:2404.13841*, 2024.
 - [14] A. Singh, P. Vepakomma, O. Gupta, and R. Raskar, “detailed comparison of communication efficiency of split learning and federated learning,” *arXiv preprint arXiv:1909.09145*, 2019.
 - [15] J. Nguyen, K. Malik, M. Sanjabi, and M. Rabbat, “Where to begin? exploring the impact of pre-training and initialization in federated learning,” *arXiv preprint arXiv:2206.15387*, 2022.
 - [16] S. Dayal, D. Alhadidi, A. Abbasi Tadi, and N. Mohammed, “Comparative analysis of membership inference attacks in federated learning,” in *Proceedings of the 27th International Database Engineered Applications Symposium*, pp. 185–192, 2023.
 - [17] H. Hu, Z. Salcic, L. Sun, G. Dobbie, P. S. Yu, and X. Zhang, “Membership inference attacks on machine learning: A survey,” *ACM Computing Surveys (CSUR)*, vol. 54, no. 11s, pp. 1–37, 2022.
 - [18] X. Wang, N. Wang, L. Wu, Z. Guan, X. Du, and M. Guizani, “Gbmia: Gradient-based membership inference attack in federated learning,” in *ICC 2023-IEEE International Conference on Communications*, pp. 5066–5071, IEEE, 2023.
 - [19] M. Fredrikson, S. Jha, and T. Ristenpart, “Model inversion attacks that exploit confidence information and basic countermeasures,” in *Proceedings of the 22nd ACM SIGSAC conference on computer and communications security*, pp. 1322–1333, 2015.

- [20] J. Li, A. S. Rakin, X. Chen, Z. He, D. Fan, and C. Chakrabarti, “Ressfl: A resistance transfer framework for defending model inversion attack in split federated learning,” in *Proceedings of the IEEE/CVF Conference on Computer Vision and Pattern Recognition*, pp. 10194–10202, 2022.
- [21] Y. Zhang, R. Jia, H. Pei, W. Wang, B. Li, and D. Song, “The secret revealer: Generative model-inversion attacks against deep neural networks,” in *Proceedings of the IEEE/CVF conference on computer vision and pattern recognition*, pp. 253–261, 2020.
- [22] E. Bagdasaryan, A. Veit, Y. Hua, D. Estrin, and V. Shmatikov, “How to backdoor federated learning,” in *International conference on artificial intelligence and statistics*, pp. 2938–2948, PMLR, 2020.
- [23] T. Kim, J. Li, N. Madaan, S. Singh, and C. Joe-Wong, “Adversarial robustness unhardening via backdoor attacks in federated learning,” in *NeurIPS 2023 Workshop on Backdoors in Deep Learning-The Good, the Bad, and the Ugly*, 2023.
- [24] J. Yu, Y. Wang, C. Zhao, B. Ghanem, and J. Zhang, “Freedom: Training-free energy-guided conditional diffusion model,” in *Proceedings of the IEEE/CVF International Conference on Computer Vision (ICCV)*, pp. 23174–23184, October 2023.
- [25] S. Pranav and J. M. Moura, “Peer-to-peer learning+ consensus with non-iid data,” in *2023 57th Asilomar Conference on Signals, Systems, and Computers*, pp. 709–713, IEEE, 2023.
- [26] Y. Zhao, M. Li, L. Lai, N. Suda, D. Civin, and V. Chandra, “Federated learning with non-iid data,” *arXiv preprint arXiv:1806.00582*, 2018.
- [27] Z. Li, K. Ren, X. Jiang, B. Li, H. Zhang, and D. Li, “Domain generalization using pretrained models without fine-tuning,” *arXiv preprint arXiv:2203.04600*, 2022.
- [28] Y. Tan, G. Long, J. Ma, L. Liu, T. Zhou, and J. Jiang, “Federated learning from pre-trained models: A contrastive learning approach,” *Advances in Neural Information Processing Systems*, vol. 35, pp. 19332–19344, 2022.

- [29] P. Xu, X. Zhu, and D. A. Clifton, “Multimodal learning with transformers: A survey,” *IEEE Transactions on Pattern Analysis and Machine Intelligence*, vol. 45, no. 10, pp. 12113–12132, 2023.
- [30] T. Kenneweg, P. Kenneweg, and B. Hammer, “Foundation model vision transformers are great tracking backbones,” in *2024 International Conference on Artificial Intelligence, Computer, Data Sciences and Applications (ACDSA)*, pp. 1–6, IEEE, 2024.
- [31] T. Li, A. K. Sahu, M. Zaheer, M. Sanjabi, A. Talwalkar, and V. Smith, “Federated optimization in heterogeneous networks,” *Proceedings of Machine learning and systems*, vol. 2, pp. 429–450, 2020.
- [32] S. I. Nikolenko, *Synthetic data for deep learning*, vol. 174. Springer, 2021.
- [33] S. P. Karimireddy, S. Kale, M. Mohri, S. Reddi, S. Stich, and A. T. Suresh, “Scaffold: Stochastic controlled averaging for federated learning,” in *International conference on machine learning*, pp. 5132–5143, PMLR, 2020.
- [34] R. Vaz, “Rome weather classification.” <https://www.kaggle.com/datasets/rogeriovaz/rome-weather-classification>, 2021. Accessed: 2024-05-21.
- [35] A. Dosovitskiy, L. Beyer, A. Kolesnikov, D. Weissenborn, X. Zhai, T. Unterthiner, M. Dehghani, M. Minderer, G. Heigold, S. Gelly, *et al.*, “An image is worth 16x16 words: Transformers for image recognition at scale,” *arXiv preprint arXiv:2010.11929*, 2020.
- [36] C. Zhou, Q. Li, C. Li, J. Yu, Y. Liu, G. Wang, K. Zhang, C. Ji, Q. Yan, L. He, *et al.*, “A comprehensive survey on pretrained foundation models: A history from bert to chatgpt,” *arXiv preprint arXiv:2302.09419*, 2023.
- [37] H. Xiao, “Weather phenomenon database (WEAPD),” 2021.
- [38] J.-I. Park and C. Joe-Wong, “Federated learning with flexible architectures,” in *Joint European Conference on Machine Learning and Knowledge Discovery in Databases*, pp. 143–161, Springer, 2024.

- [39] E. Diao, J. Ding, and V. Tarokh, “Heterofl: Computation and communication efficient federated learning for heterogeneous clients,” *arXiv preprint arXiv:2010.01264*, 2020.

Appendix Overview

This appendix provides additional details and results to complement the main text, offering further insight into the experimental setup, theoretical analysis, and security considerations for FedBaF.

The appendix is organized as follows:

Experimental Setup in Section A

This section details the experimental configurations, including data distributions, network architectures for vision and language tasks, and hyper-parameters under IID and non-IID settings.

Formulas for Evaluating Computational Complexity in Section B

We present the mathematical formulas used to compute the computational complexity of the FedBaF algorithm, specifically focusing on multiply-accumulate (MAC) operations across clients and training rounds.

Additional Experimental Evaluations in Section C

This section includes supplementary experimental results, analyzing the effect of varying foundation model quality on FedBaF’s performance and comparisons using the official pre-trained foundation model. Computational complexity is also compared to scenarios without foundation models and weight initialization.

Training Curves in Section D

We provide training curves that display the progression of model accuracy over training epochs for the Pre-ResNet and Vision Transformer models, illustrating comparisons between FedBaF, weight initialization, and without foundation model cases under IID and non-IID conditions.

Convergence Analysis in Section E

This section provides a theoretical analysis of FedBaF’s convergence properties, detailing how the algorithm performs under different client data distributions and demonstrating the theoretical

guarantees for its performance.

Proofs of Propositions in Section F

In this section, we include the formal proofs of Propositions 1 and 2, outlined in the theoretical analysis in Section 4, which support the claims made regarding FedBaF’s performance and convergence behavior.

Security Analysis in the Presence of Adversarial Attacks in Section G

This section provides an in-depth security analysis of FedBaF, focusing on its robustness against adversarial attacks such as misclassification and backdoor attacks. We compare FedBaF’s resilience to malicious clients with traditional methods, showing how FedBaF mitigates the negative impact of attacks and preserves global model integrity.

A Experimental Setup

Table 1: The specific conditions under which our experiments were conducted, including data distribution and model training settings.

Evaluation	Pretrained Model Training			Performance Comparison						
				From Tiny ImageNet-200		From Weather Image		From WikiText-2	From ImageNet (PyTorch)	
				IID	Non-IID	IID	Non-IID	-	IID	Non-IID
Number of clients	1			100		10		100	100	
Fraction of active clients C	1			0.1						
Number of classes for each client	100	11	-	10	2	5	2	-	10	2
Number of samples for each client	50,000 ~ 100,000	2,500 ~ 5,000	640,000 ~ 1,280,000	125 ~ 250		10 ~ 20		7,680 ~ 8960	125 ~ 250	
Data	Tiny ImageNet-200	Weather Image	WikiText-2	CIFAR-10		Rome Weather Image		Penn Treebank	CIFAR-10	
Model	Pre-ResNet	Vision Transformer	Transformer	Pre-ResNet		Vision Transformer		Transformer	Vision Transformer	
Local epochs E	300	300	300	5						
Local mini-batch size B	128			50		50		128	125	
Communication rounds	1			200	250	200	250	200	200	250
Optimizer	SGD									
Momentum	0.9									
Weight decay	1e-4									
Learning rate η	0.1			0.01		0.01		0.1	0.01	
Learning rate 0.1x decay schedule	[150, 225]	[150, 225]	Not applied	Not applied						
Batch normalization layer	Non-static									
μ for proximal term in FedProx	Not applied			0.01				Not applied	0.01	

In this section, we provide details about our experimental setup and network architectures. For vision tasks using Pre-ResNets and Vision Transformers, we conduct evaluations in both IID and non-IID environments. In **IID settings**, each client’s data distribution is uniform across all classes, with an equal number of samples from each class. In **non-IID settings**, clients receive samples from only 20% of the dataset’s classes for CIFAR-10 and 50% of the dataset’s classes for Rome Weather Image, but maintain an equal number of samples for each class they have. *During local training in these settings, clients zero out logits for classes not present in their data.* For language tasks using Transformers, each client has specific numbers of tokenized words grouped sequentially. Details of the experimental settings can be found in Table 1.

For the network architecture configuration, details for Pre-ResNets and Transformers can be found in Table 2. For Vision Transformer, we used the standard ViT_B-16 model with no modifications except changing the last output layers according to the new data. This model was obtained from the PyTorch library. Additionally, we also tested FedBaF with official pre-trained foundation model weights that are available online (not developed by us). We specifically used the ImageNet

pre-trained weights for a standard Vision Transformer from PyTorch’s official model repository: (ViT_B_16_Weights.IMAGENET1K_SWAG_E2E_V1).

Table 2: This table presents the detailed structures of the neural networks (Pre-ResNet and Transformer) utilized in our Federated Learning experiments and making foundation models.

Model	Section 1	Section 2	Section 3	Section 4	Section 5	Section 6	Section 7	Section 8			
Pre-ResNet	$[3 \times 3, 64] \times 1$	$\begin{bmatrix} [3 \times 3, 64] \\ [3 \times 3, 64] \end{bmatrix} \times 2$	$\begin{bmatrix} [3 \times 3, 128] \\ [3 \times 3, 128] \end{bmatrix} \times 2$	$\begin{bmatrix} [3 \times 3, 256] \\ [3 \times 3, 256] \end{bmatrix} \times 2$	$\begin{bmatrix} [3 \times 3, 512] \\ [3 \times 3, 512] \end{bmatrix} \times 2$	$N_{classes}$ -d fc					
Model	Encoder				Decoder				Classifier		
	Attention	FeedForward	Attention	FeedForward		Attention	FeedForward	Attention	FeedForward		
Transformer	192-d fc 64-d fc	$\begin{bmatrix} [3 \times 3, 64] \\ [3 \times 3, 64] \end{bmatrix} \times 2$	192-d fc 64-d fc	$\begin{bmatrix} [3 \times 3, 64] \\ [3 \times 3, 64] \end{bmatrix} \times 2$	N_{token} -d fc	N_{token} -d fc	192-d fc 64-d fc	$\begin{bmatrix} [3 \times 3, 64] \\ [3 \times 3, 64] \end{bmatrix} \times 1$	192-d fc 64-d fc	$\begin{bmatrix} [3 \times 3, 64] \\ [3 \times 3, 64] \end{bmatrix} \times 1$	N_{token} -d fc

B Formulas for Evaluating Computational Complexity

In this section, we provide metrics for evaluating the computational complexity, as discussed in Section C.3.

To evaluate *computational complexity*, we track the number of multiply-accumulate (MAC) operations, denoted as MACS. MACS_k represents the number of MAC operations required to process all the local data samples held by client k . The average MAC per client, denoted as $\overline{\text{MACS}}$, is calculated by averaging the MACS values for all clients participating in a single round of FL:

$$\overline{\text{MACS}} = \frac{1}{m} \sum_{k=1}^m \text{MACS}_k$$

Here, m is the number of participating clients in the given round. For each local training epoch, the computational complexity, referred to as MACE (Multiply-Accumulate Complexity per Epoch), is calculated as:

$$\text{MACE} = m \times \tilde{n} \times \overline{\text{MACS}}.$$

Here, \tilde{n} is the median number of data samples per client. This metric reflects the computational load incurred by m clients during local training in each epoch.

To compute the total computational load for the entire FL system, denoted as TMAC (Total Multiply-Accumulate Complexity), we multiply the number of local epochs E , the number of aggregation rounds T , and the previously calculated MACE:

$$\text{TMAC} = T \times E \times \text{MACE}.$$

This provides the total number of MAC operations required for the entire training process across all clients and rounds, accounting for both the number of local epochs and the aggregation rounds in the FL system.

C Additional Experimental Evaluations

In this section, we present additional experimental results that provide further insight into the performance of FedBaF across various tasks and scenarios. These evaluations focus on the impact of different qualities of foundation models, the application of the real pre-trained foundation model, and computational complexities. We compare the use of foundation models in both IID and non-IID settings with weight initialization and cases where no foundation model is used.

C.1 Differentiating the Quality of Pre-Trained Foundation Models

Table 3: Image classification test accuracy results for Pre-ResNet using the no foundation, weight initialization, and FedBaF methods (best of 3 trials).

FedAvg										
Pre-trained Samples	Malicious Clients (ζ) Attack Intensity (λ)	IID - Global Testing Accuracy			Non-IID - Local Testing Accuracy			Non-IID - Global Testing Accuracy		
		No Foundation	Weight Initialization	FedBaF	No Foundation	Weight Initialization	FedBaF	No Foundation	Weight Initialization	FedBaF
50,000	$\zeta=0\%, \lambda=1$	82.9	84.1	84.0	95.6	98.0	98.2	57.3	68.6	69.8
	$\zeta=10\%, \lambda=1$	81.7	82.4	82.8	95.1	97.5	98.1	49.0	62.1	63.8
	$\zeta=20\%, \lambda=1$	80.1	81.0	82.0	94.0	97.3	97.6	43.6	57.3	58.2
	$\zeta=50\%, \lambda=1$	73.0	78.2	78.6	85.9	90.3	91.3	39.4	56.6	57.7
	$\zeta=50\%, \lambda=5$	73.1	78.7	79.0	87.7	93.4	94.0	35.4	56.6	58.3
100,000	$\zeta=0\%, \lambda=1$	82.9	85.9	85.9	95.6	98.4	98.6	57.3	71.9	73.4
	$\zeta=10\%, \lambda=1$	81.7	84.3	84.8	95.1	98.0	98.3	49.0	64.2	67.0
	$\zeta=20\%, \lambda=1$	80.1	83.5	83.7	94.0	97.5	97.9	43.6	59.8	61.9
	$\zeta=50\%, \lambda=1$	73.0	80.6	80.8	85.9	91.1	92.0	39.4	60.1	60.8
	$\zeta=50\%, \lambda=5$	73.1	80.6	80.8	87.7	94.0	94.8	35.4	56.4	61.0
FedProx										
Pre-trained Samples	Malicious Clients (ζ) Attack Intensity (λ)	IID - Global Testing Accuracy			Non-IID - Local Testing Accuracy			Non-IID - Global Testing Accuracy		
		No Foundation	Weight Initialization	FedBaF	No Foundation	Weight Initialization	FedBaF	No Foundation	Weight Initialization	FedBaF
50,000	$\zeta=0\%, \lambda=1$	82.8	84.2	84.1	95.4	98.0	98.2	57.0	68.6	69.9
	$\zeta=10\%, \lambda=1$	81.5	82.4	82.9	95.4	97.5	98.2	49.8	62.1	63.7
	$\zeta=20\%, \lambda=1$	80.1	81.1	82.0	94.0	97.4	97.6	45.0	57.3	58.1
	$\zeta=50\%, \lambda=1$	73.5	78.0	78.7	87.6	90.3	91.5	40.8	56.7	57.7
	$\zeta=50\%, \lambda=5$	73.5	78.4	78.7	88.0	93.2	94.0	35.7	56.8	58.5
100,000	$\zeta=0\%, \lambda=1$	82.8	85.9	85.8	95.4	98.4	98.6	57.0	71.9	73.4
	$\zeta=10\%, \lambda=1$	81.5	84.4	84.8	95.4	98.0	98.3	49.8	64.4	67.3
	$\zeta=20\%, \lambda=1$	80.1	83.8	84.0	94.0	97.6	97.9	45.0	59.8	61.9
	$\zeta=50\%, \lambda=1$	73.5	80.5	80.6	87.6	90.9	92.3	40.8	59.9	60.7
	$\zeta=50\%, \lambda=5$	73.5	80.5	80.9	88.0	94.6	94.8	35.7	55.1	60.5

We conducted experiments to evaluate the generalized performance of FedBaF by varying the quality of foundation models. Tables 3, 4, and 5 present the results for image classification tasks using Pre-ResNet and Vision Transformer models, as well as a next-word prediction task using a Transformer model.

To assess the impact of foundation model quality, we varied the number of pre-trained samples used for each model and assessed each method’s performance under a varying number of malicious clients and attack intensity. Interestingly, larger sample sizes do not always lead to better results, as seen in Table 3, where excessive pre-training can negatively impact performance. This trend is

Table 4: Image classification test accuracy results for Vision Transformer using no foundation, weight initialization, and FedBaF methods (best of 3 trials).

FedAvg										
Pre-trained Samples	Malicious Clients (ζ) Attack Intensity (λ)	IID - Global Testing Accuracy			Non-IID - Local Testing Accuracy			Non-IID - Global Testing Accuracy		
		No Foundation	Weight Initialization	FedBaF	No Foundation	Weight Initialization	FedBaF	No Foundation	Weight Initialization	FedBaF
2,500	$\zeta=0\%, \lambda=1$	74.0	82.0	82.0	93.4	99.1	98.9	64.0	76.0	88.0
	$\zeta=10\%, \lambda=1$	72.0	78.0	80.0	94.9	96.7	96.8	62.0	72.0	82.0
	$\zeta=20\%, \lambda=1$	72.0	74.0	78.0	91.4	96.7	94.0	58.0	74.0	74.0
	$\zeta=50\%, \lambda=1$	72.0	70.0	74.0	90.3	91.4	92.0	60.0	64.0	66.0
	$\zeta=50\%, \lambda=5$	50.0	70.0	78.0	91.4	91.3	89.7	50.0	62.0	66.0
5,000	$\zeta=0\%, \lambda=1$	74.0	72.0	72.0	93.4	98.0	98.0	64.0	78.0	76.0
	$\zeta=10\%, \lambda=1$	72.0	72.0	74.0	94.9	94.3	93.9	62.0	74.0	76.0
	$\zeta=20\%, \lambda=1$	72.0	78.0	72.0	91.4	90.6	92.0	58.0	72.0	68.0
	$\zeta=50\%, \lambda=1$	72.0	68.0	68.0	90.3	92.3	90.0	60.0	64.0	68.0
	$\zeta=50\%, \lambda=5$	50.0	72.0	70.0	91.4	92.3	90.5	50.0	66.0	66.0
FedProx										
Pre-trained Samples	Malicious Clients (ζ) Attack Intensity (λ)	IID - Global Testing Accuracy			Non-IID - Local Testing Accuracy			Non-IID - Global Testing Accuracy		
		No Foundation	Weight Initialization	FedBaF	No Foundation	Weight Initialization	FedBaF	No Foundation	Weight Initialization	FedBaF
2,500	$\zeta=0\%, \lambda=1$	76.0	82.0	82.0	93.5	99.1	98.9	64.0	76.0	88.0
	$\zeta=10\%, \lambda=1$	76.0	78.0	80.0	95.0	96.7	96.8	64.0	72.0	82.0
	$\zeta=20\%, \lambda=1$	74.0	74.0	78.0	91.3	96.7	94.0	58.0	74.0	74.0
	$\zeta=50\%, \lambda=1$	62.0	70.0	74.0	89.2	91.4	92.0	56.0	64.0	66.0
	$\zeta=50\%, \lambda=5$	50.0	70.0	78.0	90.3	91.3	89.7	48.0	62.0	66.0
5,000	$\zeta=0\%, \lambda=1$	76.0	72.0	72.0	93.5	98.0	98.0	64.0	78.0	76.0
	$\zeta=10\%, \lambda=1$	76.0	72.0	74.0	95.0	94.3	93.9	64.0	74.0	76.0
	$\zeta=20\%, \lambda=1$	74.0	78.0	72.0	91.3	90.6	92.0	58.0	72.0	68.0
	$\zeta=50\%, \lambda=1$	62.0	68.0	68.0	89.2	92.3	90.0	56.0	64.0	68.0
	$\zeta=50\%, \lambda=5$	50.0	72.0	70.0	90.3	92.3	90.5	48.0	66.0	66.0

Table 5: Next-word prediction perplexity results for Transformer models using no foundation, weight initialization, and FedBaF methods (best of 3 trials). **Lower perplexity is better.**

FedAvg				
Pre-trained Samples	Malicious Clients (ζ) Attack Intensity (λ)	Global Testing Perplexity		
		No Foundation	Weight Initialization	FedBaF
640,000	$\zeta=0\%, \lambda=1$	536.5	172.8	128.6
	$\zeta=10\%, \lambda=1$	549.4	191.8	137.8
	$\zeta=20\%, \lambda=1$	531.3	213.7	159.4
	$\zeta=50\%, \lambda=1$	501.6	330.6	298.4
	$\zeta=50\%, \lambda=5$	680.4	311.7	275.1
1,280,000	$\zeta=0\%, \lambda=1$	536.5	202.6	183.3
	$\zeta=10\%, \lambda=1$	549.4	227.3	201.4
	$\zeta=20\%, \lambda=1$	531.3	258.3	224.2
	$\zeta=50\%, \lambda=1$	501.6	371.9	337.3
	$\zeta=50\%, \lambda=5$	680.4	343.9	322.8

further evidenced in Tables 4, 5. The reason behind this is likely due to overfitting or reduced adaptability to new tasks. Despite these variations, FedBaF consistently outperforms models without foundation models and delivers similar testing performance to weight initialization.

Training curves for selected cases can be found in Section D.

C.2 Using the Official Pre-Trained Foundation Model

We also evaluated the performance of FedBaF using the official pre-trained foundation model that was not developed by us. Specifically, we used ImageNet pre-trained weights for the Vision Trans-

Table 6: Image classification test accuracy results for Vision Transformer using official pre-trained foundation model weights from PyTorch. Comparisons are made between no foundation model, weight initialization, and FedBaF methods (best of 3 trials).

FedAvg										
Pre-trained Samples	Malicious Clients (ζ) Attack Intensity (λ)	IID - Global Testing Accuracy			Non-IID - Local Testing Accuracy			Non-IID - Global Testing Accuracy		
		No Foundation	Weight Initialization	FedBaF	No Foundation	Weight Initialization	FedBaF	No Foundation	Weight Initialization	FedBaF
1,281,167	$\zeta=0\%, \lambda=1$	47.9	81.5	81.3	84.2	96.9	96.0	41.3	70.8	71.5
	$\zeta=10\%, \lambda=1$	47.6	81.2	80.5	85.5	96.3	96.6	38.6	67.0	68.7
	$\zeta=20\%, \lambda=1$	45.6	80.3	80.1	85.0	94.9	94.1	36.3	63.7	65.4
	$\zeta=50\%, \lambda=1$	42.3	77.2	76.4	73.7	83.3	80.4	33.7	49.8	51.4
	$\zeta=50\%, \lambda=5$	37.8	74.3	72.7	74.7	85.6	82.4	28.7	40.4	50.4
FedProx										
Pre-trained Samples	Malicious Clients (ζ) Attack Intensity (λ)	IID - Global Testing Accuracy			Non-IID - Local Testing Accuracy			Non-IID - Global Testing Accuracy		
		No Foundation	Weight Initialization	FedBaF	No Foundation	Weight Initialization	FedBaF	No Foundation	Weight Initialization	FedBaF
1,281,167	$\zeta=0\%, \lambda=1$	47.4	80.9	80.5	78.3	89.0	87.3	41.2	68.7	71.2
	$\zeta=10\%, \lambda=1$	46.7	80.4	80.3	75.9	85.5	83.1	37.7	61.0	62.2
	$\zeta=20\%, \lambda=1$	45.1	79.4	79.7	73.1	81.1	79.2	35.4	59.0	59.7
	$\zeta=50\%, \lambda=1$	41.7	76.7	75.9	62.5	64.9	64.9	32.8	48.8	49.2
	$\zeta=50\%, \lambda=5$	36.8	73.5	69.8	63.9	66.6	67.4	28.5	37.3	46.5

former model, obtained from PyTorch’s official model repository. As shown in Table 6, FedBaF outperforms scenarios without foundation models and delivers similar performance to weight initialization using pre-trained weights. These results demonstrate that FedBaF can effectively integrate widely adopted pre-trained models.

C.3 Computational Complexity

Table 7: Pre-ResNet and Vision Transformer computational complexities using no foundation model, weight initialization, and FedBaF methods. **Note: T represents trillion.**

a) Pre-ResNet

	Pre-trained Samples	IID			Non-IID		
		No Foundation	Weight Initialization	FedBaF	No Foundation	Weight Initialization	FedBaF
FedAvg	50,000	1.51 T	0.20 T	0.18 T	2.63 T	0.26 T	0.27 T
	100,000	1.51 T	0.11 T	0.13 T	2.63 T	0.21 T	0.20 T
FedProx	50,000	1.52 T	0.21 T	0.18 T	2.64 T	0.26 T	0.27 T
	100,000	1.52 T	0.11 T	0.13 T	2.64 T	0.21 T	0.20 T

b) Vision Transformer

	Pre-trained Samples	IID			Non-IID		
		No Foundation	Weight Initialization	FedBaF	No Foundation	Weight Initialization	FedBaF
FedAvg	2,500	7.34 T	0.20 T	0.23 T	8.08 T	0.20 T	0.49 T
	5,000	7.34 T	0.26 T	0.20 T	8.08 T	0.14 T	0.26 T
FedProx	2,500	6.66 T	0.20 T	0.23 T	8.91 T	0.20 T	0.49 T
	5,000	6.66 T	0.26 T	0.20 T	8.91 T	0.14 T	0.26 T

FedBaF demonstrates remarkable efficiency in terms of computational complexity, requiring significantly fewer computations than scenarios without foundation models and performing similarly to weight initialization methods.

To demonstrate that FedBaF’s computational demands are minimal, even when integrating the foundation model in every training round, we assess its computational complexity. Table 7 presents the computational complexities, measured in TMAC (Total Multiply-Accumulate Operations) from Section B, for six non-adversarial scenarios in both IID and non-IID settings. To calculate these complexities, we consider the number of training rounds required to achieve specific global testing accuracies: 75% for IID and 50% for non-IID scenarios in Pre-ResNet cases. For Vision Transformer cases, we set the thresholds to 60% IID accuracy and 60% non-IID accuracy.

Compared to the no weight initialization cases, **FedBaF requires significantly fewer computations** across both IID and non-IID scenarios. Specifically, for Pre-ResNet IID and non-IID cases, computations are reduced by 88.1-91.4% and 89.7-92.4% for FedAvg, and by 88.2-91.4% and 89.8-92.4% for FedProx, respectively. Similarly, for Vision Transformer, IID and non-IID scenarios see a reduction of 96.9-97.3% and 93.9-96.8% for FedAvg, and 96.5-97.0% and 94.5-97.1% for FedProx in computations. Therefore, these findings indicate that FedBaF’s computational demands are relatively minimal despite the foundation model being integrated into every training round.

These findings clearly indicate that **FedBaF’s computational demands are minimal**, even when integrating the foundation model into every training round, making it a highly efficient

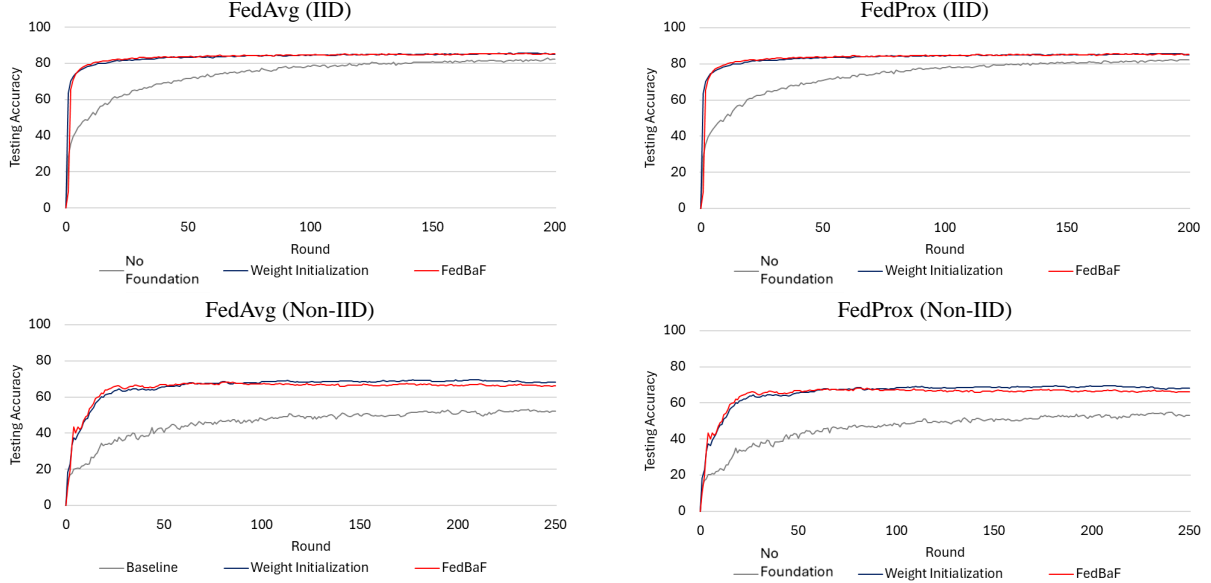
solution in both IID and non-IID environments.

D Training curves

In this section, we present the evolution of model accuracy over epochs for the experiments described in Section C, as shown in Figure 6. The experiments involve both Pre-ResNet and Vision Transformer models, focusing on two setups: **1) Pre-ResNet**, with foundation models pre-trained using TinyImageNet-200 (50,000 pre-trained samples), and **2) Vision Transformer**, with foundation models pre-trained using the Weather Image dataset (2,500 pre-trained samples). We present results for both IID and non-IID settings, using FedAvg and FedProx as the aggregation methods.

These training curves illustrate the progression of model accuracy throughout the training process, comparing the behaviors of models using weight initialization and FedBaF. The curves demonstrate that FedBaF performs similarly to traditional weight initialization methods and achieves higher accuracies than when no foundation model is used.

a) Pre-ResNet (From TinyImageNet-200; 50,000 pre-trained samples)



b) Vision Transformer (From Weather Image; 2,500 pre-trained samples)

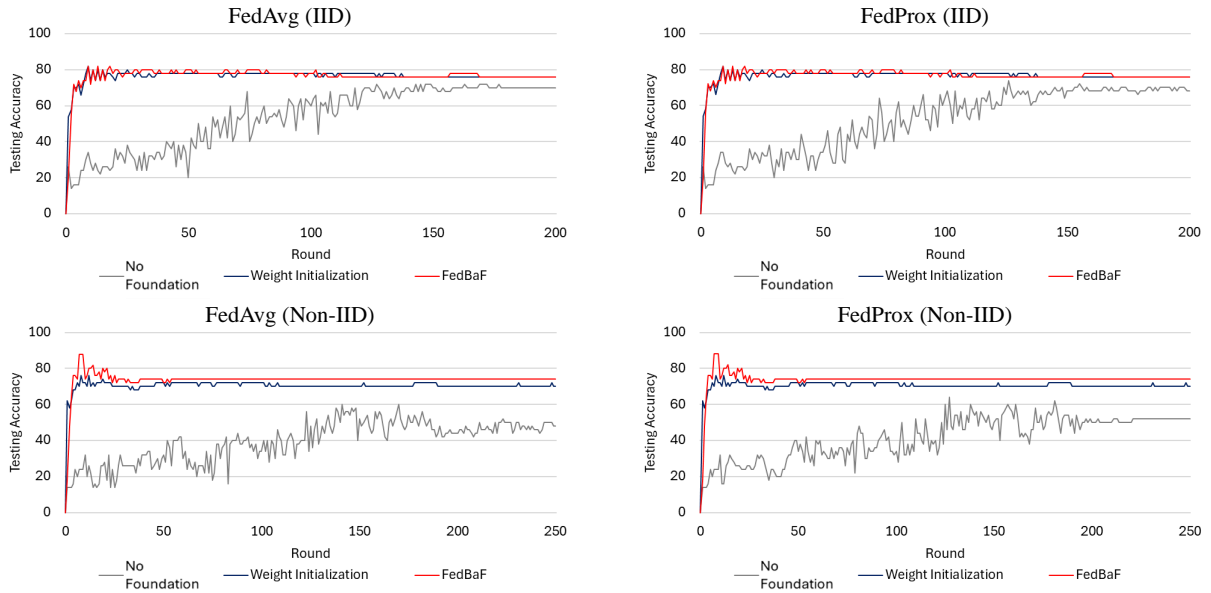


Figure 6: This figure shows the evolution of model accuracy over training epochs for Pre-ResNets and Vision Transformers under IID and Non-IID scenarios. It compares the performance using no foundation model, weight initialization, and FedBaF with FedAvg and FedProx.

E Convergence Analysis

This section provides a convergence analysis for the FedBaF algorithm under non-convex settings using Stochastic Gradient Descent (SGD). The study demonstrates how integrating a foundation model during aggregation can improve convergence rates, even in non-IID scenarios.

E.1 Problem Setup

Consider the global objective function in federated learning, which is defined as:

$$F(\mathbf{w}) = \frac{1}{\sum_{k=1}^m n_k} \sum_{k=1}^m n_k f_{D_k}(\mathbf{w}), \quad (3)$$

where m is the number of clients, $f_{D_k}(\mathbf{w})$ represents the local objective function on client k , n_k is the number of data samples at client k , $\mathbf{w} \in \mathbb{R}^d$ are the model weights, $F(\mathbf{w})$ is the global objective function. *To simplify our analysis, we assume all clients participate in every global round.*

We define $\mathbf{w}_k^{(t,\ell)}$ as the model weights of client k at global round t and local update step ℓ . Therefore, before the first local update step in each global round, each client's model weights \mathbf{w}_k^t are equal to the global model weights \mathbf{w}_t and

$$\mathbf{w}_k^{(t,0)} = \mathbf{w}_k^t = \mathbf{w}_t. \quad (4)$$

E.1.1 Assumptions

We make the following standard assumptions to facilitate the convergence analysis:

L-Smoothness: Each local objective function $f_{D_k}(\mathbf{w})$ is L -smooth with respect to \mathbf{w} , meaning:

$$f_{D_k}(\mathbf{v}) \leq f_{D_k}(\mathbf{w}) + \nabla f_{D_k}(\mathbf{w})^\top (\mathbf{v} - \mathbf{w}) + \frac{L}{2} \|\mathbf{v} - \mathbf{w}\|^2, \quad \forall \mathbf{w}, \mathbf{v} \in \mathbb{R}^d. \quad (5)$$

and

$$\|\nabla f_{D_k}(\mathbf{v}) - \nabla f_{D_k}(\mathbf{w})\| \leq L \|\mathbf{v} - \mathbf{w}\|, \quad \forall \mathbf{w}, \mathbf{v} \in \mathbb{R}^d. \quad (6)$$

Unbiased Mini-Batch Gradients: The stochastic gradients computed over mini-batches during local updates are unbiased estimates of the true gradients.

$$\mathbb{E}[g_{D_k}(\mathbf{w}; b)] = \nabla f_{D_k}(\mathbf{w}) \quad \forall \mathbf{w} \in \mathbb{R}^d. \quad (7)$$

Bounded Gradient Norm: The gradients of the local objective functions are bounded by a constant β . Specifically,

$$\|\nabla f_{D_k}(\mathbf{w})\| \leq \beta \quad \forall \mathbf{w} \in \mathbb{R}^d. \quad (8)$$

Bounded Gradient Noise:

$$\mathbb{E} \left[\|g_{D_k}(\mathbf{w}_k^{(t,\ell)}; b_{k,\ell})\|^2 \right] \leq G^2 + B^2 \|\nabla F(\mathbf{w}_t)\|^2 \quad (9)$$

where G^2 and B^2 are constants that bound the dissimilarity, $b_{k,\ell}$ denotes the j -th mini-batch on client k , and ℓ indexes the local update steps during global round t .

E.2 FedBaF Aggregation Step with Multiple Local Updates

The FedBaF algorithm operates in global rounds, where each global round t includes multiple local iterations denoted by ℓ . Each client performs multiple local updates in each global round.

The global model is updated at round t using the rule:

$$\mathbf{w}_{t+1} = \frac{1}{1 + \alpha_t \tau_t} (\mathbf{w}'_t + \alpha_t \tau_t \mathbf{w}_{\text{pre}}), \quad (10)$$

where \mathbf{w}'_t is the aggregated model from the client updates, \mathbf{w}_{pre} is the foundation model's weights, α_t is a scaling factor, and τ_t represents the correction factor based on the foundation model.

Each client k performs multiple local SGD updates over local iterations $\ell = 0, 1, \dots, \Lambda_k - 1$, where Λ_k is the number of local updates for each client k . For each local update, the local model is updated as:

$$\mathbf{w}_k^{(t,\ell+1)} = \mathbf{w}_k^{(t,\ell)} - \eta g_{D_k}(\mathbf{w}_k^{(t,\ell)}; b_{k,\ell}), \quad (11)$$

where $g_{D_k}(\mathbf{w}_k^{(t,\ell)}; b_{k,\ell})$ is the stochastic gradient computed on the mini-batch $b_{k,\ell}$ at local iteration

ℓ .

At the end of the local updates, each client sends the model $\mathbf{w}_k^{(t, \Lambda_k)}$ to the server, where the global model \mathbf{w}'_t is computed as the weighted average of the client updates:

$$\mathbf{w}'_t = \mathbf{w}_t - \eta \sum_{k=1}^m p_k \sum_{\ell=0}^{\Lambda_k-1} g_{D_k}(\mathbf{w}_k^{(t, \ell)}; b_{k, \ell}), \quad (12)$$

where $p_k = \frac{n_k}{\sum_{k=1}^m n_k}$ is the weight of client k .

Substituting this into the FedBaF update rule:

$$\mathbf{w}_{t+1} = \frac{1}{1 + \alpha_t \tau_t} \left(\mathbf{w}_t + \alpha_t \tau_t \mathbf{w}_{\text{pre}} - \eta \sum_{k=1}^m p_k \sum_{\ell=0}^{\Lambda_k-1} g_{D_k}(\mathbf{w}_k^{(t, \ell)}; b_{k, \ell}) \right) \quad (13)$$

For small values of $\alpha_t \tau_t \ll 1$, we use the fact that:

$$\begin{aligned} \frac{1}{1 + \alpha_t \tau_t} &= \sum_{i=0}^{\infty} (-\alpha_t \tau_t)^i \\ &= 1 - \alpha_t \tau_t + \sum_{i=2}^{\infty} (-\alpha_t \tau_t)^i \\ &\approx 1 - \alpha_t \tau_t \end{aligned} \quad (14)$$

which simplifies the update rule to:

$$\begin{aligned} \mathbf{w}_{t+1} &\approx \mathbf{w}_t - \eta \sum_{k=1}^m p_k \sum_{\ell=0}^{\Lambda_k-1} g_{D_k}(\mathbf{w}_k^{(t, \ell)}; b_{k, \ell}) \\ &\quad - \alpha_t \tau_t \left(\left[\mathbf{w}_t - \eta \sum_{k=1}^m p_k \sum_{\ell=0}^{\Lambda_k-1} g_{D_k}(\mathbf{w}_k^{(t, \ell)}; b_{k, \ell}) \right] - (1 - \alpha_t \tau_t) \mathbf{w}_{\text{pre}} \right). \end{aligned} \quad (15)$$

The update rule can now be interpreted as multiple local gradient descent steps combined with a bias correction. Here, we define the correction term χ_t as follows:

$$\chi_t = \alpha_t \tau_t \left(\left[\mathbf{w}_t - \eta \sum_{k=1}^m p_k \sum_{\ell=0}^{\Lambda_k-1} g_{D_k}(\mathbf{w}_k^{(t, \ell)}; b_{k, \ell}) \right] - (1 - \alpha_t \tau_t) \mathbf{w}_{\text{pre}} \right). \quad (16)$$

χ_t acts as a correction that adjusts the direction of the gradient descent to leverage the foundation

model's knowledge. The update rule becomes:

$$\mathbf{w}_{t+1} \approx \mathbf{w}_t - \eta \sum_{k=1}^m p_k \sum_{\ell=0}^{\Lambda_k-1} g_{D_k}(\mathbf{w}_k^{(t,\ell)}; b_{k,\ell}) - \chi_t. \quad (17)$$

E.3 Decrease in Objective Function

Using the smoothness property of $F(\mathbf{w})$:

$$F(\mathbf{w}_{t+1}) \leq F(\mathbf{w}_t) + \nabla F(\mathbf{w}_t)^\top (\mathbf{w}_{t+1} - \mathbf{w}_t) + \frac{L}{2} \|\mathbf{w}_{t+1} - \mathbf{w}_t\|^2. \quad (18)$$

We substitute the update rule:

$$\mathbf{w}_{t+1} - \mathbf{w}_t \approx -\eta \sum_{k=1}^m p_k \sum_{\ell=0}^{\Lambda_k-1} g_{D_k}(\mathbf{w}_k^{(t,\ell)}; b_{k,\ell}) - \chi_t. \quad (19)$$

Thus:

$$\begin{aligned} F(\mathbf{w}_{t+1}) &\lesssim F(\mathbf{w}_t) - \eta \nabla F(\mathbf{w}_t)^\top \sum_{k=1}^m p_k \sum_{\ell=0}^{\Lambda_k-1} g_{D_k}(\mathbf{w}_k^{(t,\ell)}; b_{k,\ell}) - \nabla F(\mathbf{w}_t)^\top \chi_t \\ &\quad + \frac{L}{2} \left\| \eta \sum_{k=1}^m p_k \sum_{\ell=0}^{\Lambda_k-1} g_{D_k}(\mathbf{w}_k^{(t,\ell)}; b_{k,\ell}) - \chi_t \right\|^2. \end{aligned} \quad (20)$$

Given the update rule, the change in the objective function can be bounded using the triangle inequality:

$$\begin{aligned} F(\mathbf{w}_{t+1}) - F(\mathbf{w}_t) &\lesssim -\eta \nabla F(\mathbf{w}_t)^\top \sum_{k=1}^m p_k \sum_{\ell=0}^{\Lambda_k-1} g_{D_k}(\mathbf{w}_k^{(t,\ell)}; b_{k,\ell}) - \nabla F(\mathbf{w}_t)^\top \chi_t \\ &\quad + L\eta^2 \left\| \sum_{k=1}^m p_k \sum_{\ell=0}^{\Lambda_k-1} g_{D_k}(\mathbf{w}_k^{(t,\ell)}; b_{k,\ell}) \right\|^2 + L\|\chi_t\|^2 \end{aligned} \quad (21)$$

E.3.1 Taking Expectations

We now take expectations of both sides of (21), based on the unbiasedness of mini-batch gradients and the assumptions about bounded gradient norms and smoothness.

We now compute the expectation of the change in the objective function:

$$\begin{aligned}
& \mathbb{E} \left[\nabla F(\mathbf{w}_t)^\top \left(-\eta \sum_{k=1}^m p_k \sum_{\ell=0}^{\Lambda_k-1} g_{D_k}(\mathbf{w}_k^{(t,\ell)}; b_{k,\ell}) \right) \right] \\
&= \nabla F(\mathbf{w}_t)^\top \left(-\eta \left(\sum_{k=1}^m p_k \Lambda_k \right) \nabla F(\mathbf{w}_t) + \eta \left(\sum_{k=1}^m p_k \Lambda_k \right) \nabla F(\mathbf{w}_t) - \eta \sum_{k=1}^m p_k \sum_{\ell=0}^{\Lambda_k-1} \mathbb{E} \left[g_{D_k}(\mathbf{w}_k^{(t,\ell)}; b_{k,\ell}) \right] \right) \\
&= -\eta \left(\sum_{k=1}^m p_k \Lambda_k \right) \|\nabla F(\mathbf{w}_t)\|^2 + \nabla F(\mathbf{w}_t)^\top \left(\eta \left(\sum_{k=1}^m p_k \Lambda_k \right) \sum_{k=1}^m p_k \nabla f_{D_k}(\mathbf{w}_t) - \eta \sum_{k=1}^m p_k \sum_{\ell=0}^{\Lambda_k-1} \nabla f_{D_k}(\mathbf{w}_k^{(t,\ell)}) \right). \tag{22}
\end{aligned}$$

Next, we simplify the remaining term:

$$\begin{aligned}
&= -\eta \left(\sum_{k=1}^m p_k \Lambda_k \right) \|\nabla F(\mathbf{w}_t)\|^2 + \eta \sum_{k=1}^m p_k \sum_{\ell=0}^{\Lambda_k-1} \nabla F(\mathbf{w}_t)^\top \left(\frac{\sum_{k=1}^m p_k \Lambda_k}{\Lambda_k} \nabla f_{D_k}(\mathbf{w}_t) - \nabla f_{D_k}(\mathbf{w}_k^{(t,\ell)}) \right) \\
&\leq -\eta \left(\sum_{k=1}^m p_k \Lambda_k \right) \|\nabla F(\mathbf{w}_t)\|^2 + \frac{\eta}{2} \sum_{k=1}^m p_k \sum_{\ell=0}^{\Lambda_k-1} \left[\|\nabla F(\mathbf{w}_t)\|^2 + \left\| \frac{\sum_{k=1}^m p_k \Lambda_k}{\Lambda_k} \nabla f_{D_k}(\mathbf{w}_t) - \nabla f_{D_k}(\mathbf{w}_k^{(t,\ell)}) \right\|^2 \right]. \tag{23}
\end{aligned}$$

Finally, using the fact that the gradient is bounded, we get:

$$\begin{aligned}
&\leq -\left(\frac{\eta}{2} \sum_{k=1}^m p_k \Lambda_k \right) \|\nabla F(\mathbf{w}_t)\|^2 + \frac{\eta}{2} \sum_{k=1}^m p_k \sum_{\ell=0}^{\Lambda_k-1} \left\| \frac{\sum_{k=1}^m p_k \Lambda_k}{\Lambda_k} \nabla f_{D_k}(\mathbf{w}_t) - \nabla f_{D_k}(\mathbf{w}_k^{(t,\ell)}) \right\|^2 \\
&\leq -\left(\frac{\eta}{2} \sum_{k=1}^m p_k \Lambda_k \right) \|\nabla F(\mathbf{w}_t)\|^2 + \frac{\eta}{2} \sum_{k=1}^m 2p_k \sum_{\ell=0}^{\Lambda_k-1} \left[\left\| \frac{\sum_{k=1}^m p_k \Lambda_k}{\Lambda_k} \nabla f_{D_k}(\mathbf{w}_t) \right\|^2 + \left\| \nabla f_{D_k}(\mathbf{w}_k^{(t,\ell)}) \right\|^2 \right] \\
&\leq -\left(\frac{\eta}{2} \sum_{k=1}^m p_k \Lambda_k \right) \|\nabla F(\mathbf{w}_t)\|^2 + \eta \beta^2 \sum_{k=1}^m p_k \left(\frac{(\sum_{k=1}^m p_k \Lambda_k)^2}{\Lambda_k} + \Lambda_k \right). \tag{24}
\end{aligned}$$

This provides a bound on the expected decrease in the global objective function.

Similarly,

$$\begin{aligned}
&\mathbb{E} \left[L\eta^2 \left\| \sum_{k=1}^m p_k \sum_{\ell=0}^{\Lambda_k-1} g_{D_k}(\mathbf{w}_k^{(t,\ell)}; b_{k,\ell}) \right\|^2 \right] \\
&\leq Lm\eta^2 \sum_{k=1}^m \mathbb{E} \left[\left\| p_k \sum_{\ell=0}^{\Lambda_k-1} g_{D_k}(\mathbf{w}_k^{(t,\ell)}; b_{k,\ell}) \right\|^2 \right] \\
&\leq Lm\eta^2 \sum_{k=1}^m p_k^2 \Lambda_k \sum_{\ell=0}^{\Lambda_k-1} \mathbb{E} \left[\left\| g_{D_k}(\mathbf{w}_k^{(t,\ell)}; b_{k,\ell}) \right\|^2 \right] \\
&\leq Lm\eta^2 \sum_{k=1}^m p_k^2 \Lambda_k^2 (G^2 + B^2 \|\nabla F(\mathbf{w}_t)\|^2) \tag{25}
\end{aligned}$$

Plugging these bounds into (21) gives

$$\begin{aligned}
\mathbb{E}[F(\mathbf{w}_{t+1}) - F(\mathbf{w}_t)] &\lesssim -\eta \nabla F(\mathbf{w}_t)^\top \sum_{k=1}^m p_k \sum_{\ell=0}^{\Lambda_k-1} g_{D_k}(\mathbf{w}_k^{(t,\ell)}; b_{k,\ell}) - \nabla F(\mathbf{w}_t)^\top \mathbb{E}[\chi_t] \\
&\quad + L\eta^2 \left\| \sum_{k=1}^m p_k \sum_{\ell=0}^{\Lambda_k-1} g_{D_k}(\mathbf{w}_k^{(t,\ell)}; b_{k,\ell}) \right\|^2 + L\mathbb{E}[\|\chi_t\|^2] \\
&\leq -\left(\frac{\eta}{2} \sum_{k=1}^m p_k \Lambda_k\right) \|\nabla F(\mathbf{w}_t)\|^2 + \eta\beta^2 \sum_{k=1}^m p_k \left(\frac{(\sum_{k=1}^m p_k \Lambda_k)^2}{\Lambda_k} + \Lambda_k\right) - \nabla F(\mathbf{w}_t)^\top \mathbb{E}[\chi_t] \\
&\quad + Lm\eta^2 \sum_{k=1}^m p_k^2 \Lambda_k^2 (G^2 + B^2 \|\nabla F(\mathbf{w}_t)\|^2) + L\mathbb{E}[\|\chi_t\|^2] \\
&\leq \left(-\frac{\eta}{2} \sum_{k=1}^m p_k \Lambda_k + B^2 Lm\eta^2 \sum_{k=1}^m p_k^2 \Lambda_k^2\right) \|\nabla F(\mathbf{w}_t)\|^2 + \eta\beta^2 \sum_{k=1}^m p_k \left(\frac{(\sum_{k=1}^m p_k \Lambda_k)^2}{\Lambda_k} + \Lambda_k\right) \\
&\quad - \nabla F(\mathbf{w}_t)^\top \mathbb{E}[\chi_t] + Lm\eta^2 \sum_{k=1}^m p_k^2 \Lambda_k^2 G^2 + L\mathbb{E}[\|\chi_t\|^2]
\end{aligned} \tag{26}$$

E.4 Summing Over Iterations

To establish a convergence result, we sum this inequality over T iterations:

$$\begin{aligned}
\sum_{t=1}^T F(\mathbf{w}_{t+1}) &\leq \sum_{t=1}^T F(\mathbf{w}_t) + \left(-\frac{\eta}{2} \sum_{k=1}^m p_k \Lambda_k + B^2 Lm\eta^2 \sum_{k=1}^m p_k^2 \Lambda_k^2\right) \sum_{t=1}^T \|\nabla F(\mathbf{w}_t)\|^2 \\
&\quad + \eta\beta^2 T \sum_{k=1}^m p_k \left(\frac{(\sum_{k=1}^m p_k \Lambda_k)^2}{\Lambda_k} + \Lambda_k\right) - \sum_{t=1}^T \nabla F(\mathbf{w}_t)^\top \mathbb{E}[\chi_t] \\
&\quad + Lm\eta^2 T \sum_{k=1}^m p_k^2 \Lambda_k^2 G^2 + L \sum_{t=1}^T \mathbb{E}[\|\chi_t\|^2]
\end{aligned} \tag{27}$$

As long as $\eta < \frac{\sum_{k=1}^m p_k \Lambda_k}{2B^2 Lm \sum_{k=1}^m p_k^2 \Lambda_k^2}$, the term $\frac{1}{2} \sum_{k=1}^m p_k \Lambda_k - B^2 Lm\eta \sum_{k=1}^m p_k^2 \Lambda_k^2$ is positive. Therefore, rearranging and dividing by T gives:

$$\begin{aligned}
\frac{1}{T} \sum_{t=1}^T \mathbb{E}[\|\nabla F(\mathbf{w}_t)\|^2] &\leq \frac{F(\mathbf{w}_1) - F(\mathbf{w}_{T+1})}{T(\frac{1}{2} \sum_{k=1}^m p_k \Lambda_k - B^2 Lm\eta \sum_{k=1}^m p_k^2 \Lambda_k^2)} \\
&\quad + \frac{\eta\beta^2 \sum_{k=1}^m p_k \left(\frac{(\sum_{k=1}^m p_k \Lambda_k)^2}{\Lambda_k} + \Lambda_k\right) + Lm\eta^2 \sum_{k=1}^m p_k^2 \Lambda_k^2 G^2}{\frac{1}{2} \sum_{k=1}^m p_k \Lambda_k - B^2 Lm\eta \sum_{k=1}^m p_k^2 \Lambda_k^2} \\
&\quad + \frac{L \sum_{t=1}^T \mathbb{E}[\|\chi_t\|^2] - \sum_{t=1}^T \nabla F(\mathbf{w}_t)^\top \mathbb{E}[\chi_t]}{T(\frac{1}{2} \sum_{k=1}^m p_k \Lambda_k - B^2 Lm\eta \sum_{k=1}^m p_k^2 \Lambda_k^2)}
\end{aligned} \tag{28}$$

If the sign of

$$L\mathbb{E}[\|\chi_t\|^2] - \nabla F(\mathbf{w}_t)^\top \mathbb{E}[\chi_t]$$

is negative, we obtain a tighter bound, which implies that the correction terms positively influence convergence.

We know that:

$$\chi_t = \alpha_t \tau_t \left(\left[\mathbf{w}_t - \eta \sum_{k=1}^m p_k \sum_{\ell=0}^{\Lambda_k-1} g_{D_k}(\mathbf{w}_k^{(t,\ell)}; b_{k,\ell}) \right] - (1 - \alpha_t \tau_t) \mathbf{w}_{\text{pre}} \right).$$

This means:

$$\mathbb{E} [\|\chi_t\|^2] = \alpha_t^2 \tau_t^2 \left\| \left[\mathbf{w}_t - \eta \sum_{k=1}^m p_k \sum_{\ell=0}^{\Lambda_k-1} \nabla f_{D_k}(\mathbf{w}_k^{(t,\ell)}) \right] - (1 - \alpha_t \tau_t) \mathbf{w}_{\text{pre}} \right\|^2.$$

Given that $\alpha_t \tau_t$ is small enough at a sufficiently large global round t , the higher-order terms with $\alpha_t^2 \tau_t^2$ become negligible. Therefore, for large t , $[\|\chi_t\|^2] \approx 0$. Next, the direction of the correction χ_t and the direction of the gradient of the global objective $\nabla F(\mathbf{w}_t)$ agreeing implies that the inner product $\nabla F(\mathbf{w}_t)^\top \mathbb{E}[\chi_t]$ is positive.

We conclude that:

$$L\mathbb{E} [\|\chi_t\|^2] < \nabla F(\mathbf{w}_t)^\top \mathbb{E}[\chi_t].$$

This shows that the variance of the correction term χ_t is significantly smaller than its impact on the inner product, leading to a tighter convergence bound, especially when $\alpha_t \tau_t$ is small but positive.

E.5 Influence of the Correction Term

The correction term χ_t , derived from the foundation model, plays a significant role in the convergence behavior. The influence of χ_t ensures that the gradient descent step is adjusted based on the foundation model's knowledge. By controlling the size of $\alpha_t \tau_t$, the foundation model can guide the global model towards better solutions, especially in non-IID scenarios. The correction term provides additional stability and enhances convergence, particularly when the local models exhibit

significant heterogeneity.

F Proofs of Propositions

F.1 Proof of Proposition 1

Proposition 1. *Let \mathbf{w}^* be a (bounded) local minimum of the global objective function in (1). Consider an FL algorithm that converges to \mathbf{w}^* and let \mathbf{w}'_t be its global model in each training round t . Suppose we run the same algorithm but using FedBaF for the aggregation, and let \mathbf{w}_t be the FedBaF global model at round t . Let α_t satisfy*

$$\alpha_t < \frac{2\|\mathbf{w}'_{t+1} - \mathbf{w}^*\|^2}{(\|\mathbf{w}_{pre} - \mathbf{w}^*\|^2 - \|\mathbf{w}'_{t+1} - \mathbf{w}^*\|^2)\tau_t} \quad (2)$$

for all t where $\|\mathbf{w}'_{t+1} - \mathbf{w}^\|^2 < \|\mathbf{w}_{pre} - \mathbf{w}^*\|^2$. Then $\forall t \|\mathbf{w}_t - \mathbf{w}^*\| < \|\mathbf{w}'_t - \mathbf{w}^*\|$.*

This means that, at any given round t , FedBaF's model weights are closer to \mathbf{w}^ .*

Proof. We present a convergence analysis of our FL framework that incorporates foundation models in the aggregation phase according to Alg. 1 *Lines 8-10*. By comparing the square distance between \mathbf{w}_{t+1} and \mathbf{w}^* to the square distance between \mathbf{w}'_{t+1} and \mathbf{w}^* , we derive conditions under which our method converges to \mathbf{w}^* faster than FedAvg. Noting that $\forall t \alpha_t, \tau_t \geq 0$,

$$\begin{aligned} \|\mathbf{w}_{t+1} - \mathbf{w}^*\|^2 &= \left\| \frac{1}{1 + \alpha_t \tau_t} (\mathbf{w}'_{t+1} + \alpha_t \tau_t \mathbf{w}_{pre}) - \mathbf{w}^* \right\|^2 \\ &= \frac{1}{(1 + \alpha_t \tau_t)^2} \|(\mathbf{w}'_{t+1} - \mathbf{w}^*) + \alpha_t \tau_t (\mathbf{w}_{pre} - \mathbf{w}^*)\|^2 \\ &\leq \frac{\|\mathbf{w}'_{t+1} - \mathbf{w}^*\|^2 + \alpha_t^2 \tau_t^2 \|\mathbf{w}_{pre} - \mathbf{w}^*\|^2}{1 + 2\alpha_t \tau_t + \alpha_t^2 \tau_t^2} \end{aligned} \quad (29)$$

For notational convenience, we define $\beta_t := \|\mathbf{w}'_{t+1} - \mathbf{w}^*\|$ and $\gamma := \|\mathbf{w}_{pre} - \mathbf{w}^*\|$. FedBaF is better than FedAvg when the right side is less than β_t^2 . So, we upper bound the right side by β_t^2 and find values of α_t that satisfy the bound.

$$\begin{aligned} \frac{\beta_t^2 + \alpha_t^2 \tau_t^2 \gamma^2}{1 + 2\alpha_t \tau_t + \alpha_t^2 \tau_t^2} &< \beta_t^2 \\ \beta_t^2 + \alpha_t^2 \tau_t^2 \gamma^2 &< \beta_t^2 + 2\alpha_t \tau_t \beta_t^2 + \alpha_t^2 \tau_t^2 \beta_t^2 \\ \alpha_t^2 \tau_t^2 (\gamma^2 - \beta_t^2) - 2\alpha_t \tau_t \beta_t^2 &< 0 \end{aligned}$$

Note that α_t is sampled from the uniform distribution $\frac{\psi}{\tau_0}\text{U}(1,2)$. For the above inequality to be satisfied for a given t , there are three cases:

1. $\beta_t > \gamma$: This case occurs when t is small and \mathbf{w}^* is closer to \mathbf{w}_{pre} than \mathbf{w}^* is to the FedBaF global model. In this case, we require

$$\alpha_t > \frac{2\beta_t^2}{(\gamma^2 - \beta_t^2)\tau_t}$$

α_t always satisfies this inequality since the RHS is negative and $\alpha_t > 0$ by definition.

2. $\beta_t = \gamma$: This means that we require $\alpha_t > 0$, which is always true by definition.
3. $\beta_t < \gamma$: This case may occur when t is large and \mathbf{w}^* is closer to the FedBaF global model than \mathbf{w}^* is to \mathbf{w}_{pre} . In this case, we get a meaningful bound for α_t :

$$\alpha_t < \frac{2\beta_t^2}{(\gamma^2 - \beta_t^2)\tau_t}$$

When $\forall t$ α_t satisfies the above conditions, the proposition holds. □

F.2 Proof of Proposition 2

Proposition 2. *Let \mathbf{w}^* be a (bounded) local minimum of the global objective function in (1). Consider an FL algorithm that converges to \mathbf{w}^* and let \mathbf{w}'_t be its global model. Consider FedBaF based on the same FL algorithm (with appropriately modified client updates and Lines 8-10 in Alg. 1) and let \mathbf{w}_t be the FedBaF global model. FedBaF's global model error has an upper bound of $\|\mathbf{w}_t - \mathbf{w}^*\| \leq \frac{\delta_t + \alpha_t \tau_t \gamma}{1 + \alpha_t \tau_t} < \delta_t$.*

Proof.

$$\begin{aligned}
\|\mathbf{w}_t - \mathbf{w}^*\| &= \left\| \frac{1}{1 + \alpha_t \tau_t} (\mathbf{w}'_t + \alpha_t \tau_t \mathbf{w}_{\text{pre}}) - \mathbf{w}^* \right\| \\
&= \frac{\|(\mathbf{w}'_t - \mathbf{w}^*) + \alpha_t \tau_t (\mathbf{w}_{\text{pre}} - \mathbf{w}^*)\|}{1 + \alpha_t \tau_t} \\
&\leq \frac{\|\mathbf{w}'_t - \mathbf{w}^*\| + \alpha_t \tau_t \|\mathbf{w}_{\text{pre}} - \mathbf{w}^*\|}{1 + \alpha_t \tau_t} \\
&= \frac{\left\| \sum_{k \in S_t} \frac{n_k}{n} (\mathbf{w}_t^k - \mathbf{w}^*) \right\| + \alpha_t \tau_t \|\mathbf{w}_{\text{pre}} - \mathbf{w}^*\|}{1 + \alpha_t \tau_t} \\
&\leq \frac{\sum_{k \in S_t} \frac{n_k}{n} \|\mathbf{w}_t^k - \mathbf{w}^*\| + \alpha_t \tau_t \|\mathbf{w}_{\text{pre}} - \mathbf{w}^*\|}{1 + \alpha_t \tau_t} \\
&\leq \frac{\delta_t + \alpha_t \tau_t \gamma}{1 + \alpha_t \tau_t}
\end{aligned}$$

where we set $\gamma = \|\mathbf{w}_{\text{pre}} - \mathbf{w}^*\|$.

Since non-IID data can cause significant variance in local updates, we compare the derived bound to FedAvg, where the bound on the distance between \mathbf{w}_t and \mathbf{w}^* is δ_t . By assumption, $\gamma \leq \delta_t$ for earlier rounds (small t). We get $\frac{\delta_t + \alpha_t \tau_t \gamma}{1 + \alpha_t \tau_t} \leq \delta_t$, which is equivalent to

$$\delta_t + \alpha_t \tau_t \gamma \leq \delta_t + \alpha_t \tau_t \delta_t = \delta_t (1 + \alpha_t \tau_t)$$

Therefore,

$$\|\mathbf{w}_t - \mathbf{w}^*\| \leq \frac{\delta_t + \alpha_t \tau_t \gamma}{1 + \alpha_t \tau_t}$$

Since $\frac{\delta_t + \alpha_t \tau_t \gamma}{1 + \alpha_t \tau_t} \leq \delta_t$, FedBaF has a tighter upper bound on $\|\mathbf{w}_t - \mathbf{w}^*\|$ than FedAvg. This demonstrates the advantage of using a foundation model in non-IID settings.

□

G Security Analysis in the Presence of Adversarial Attacks

In this section, we discuss the potential for extracting a foundation model in FedBaF and demonstrate FedBaF’s robustness against backdoor attacks. These attacks pose unique security challenges to FL systems, involving malicious alterations within model updates to degrade system performance or embed hidden vulnerabilities. We will analyze how FedBaF mitigates these threats and ensures integrity and security.

G.1 Possibility of Extracting a Foundation Model

As discussed in Section 3, using a randomized α_t prevents the extraction of the foundation model’s weights. However, the aggregated global models might still exhibit components of the foundation model by following a similar weight distribution. To investigate this, we analyze the distance between the global model and the foundation model over the first 200 aggregation rounds.

Let \mathbf{w}_{t+1} and \mathbf{w}_{pre} represent the weights of the global model and the foundation model, respectively. For each weight tensor \mathbf{w}_{t+1}^i and \mathbf{w}_{pre}^i with matching shapes, we calculate the normalized distance for each element and then average these distances. For each element j in the weight tensor \mathbf{w}_{t+1}^i and \mathbf{w}_{pre}^i :

$$\text{dist}_j^i = \frac{|w_{t+1,j}^i - w_{pre,j}^i|}{|w_{t+1,j}^i|}$$

where $w_{t+1,j}^i$ is the j -th element of the i -th weight tensor of the global model; $w_{pre,j}^i$ is the j -th element of the i -th weight tensor of the foundation model; and dist_j^i is the normalized distance for the j -th element of the i -th weight tensor.

We concatenate all element-wise distances dist_j^i across all weight tensors and then compute the mean of these distances:

$$\text{Dist} = \frac{1}{N_{param}} \sum_{i=1} \sum_{j=1} \text{dist}_j^i$$

where N_{param} is the total number of elements across all matching weight tensors and Dist is the overall average normalized distance.

In Figure 7, the curves show the distances, Dist, for each aggregation round. The minimum Dist across all cases was 1.27, indicating that the distance has a 127% scale of the magnitude of

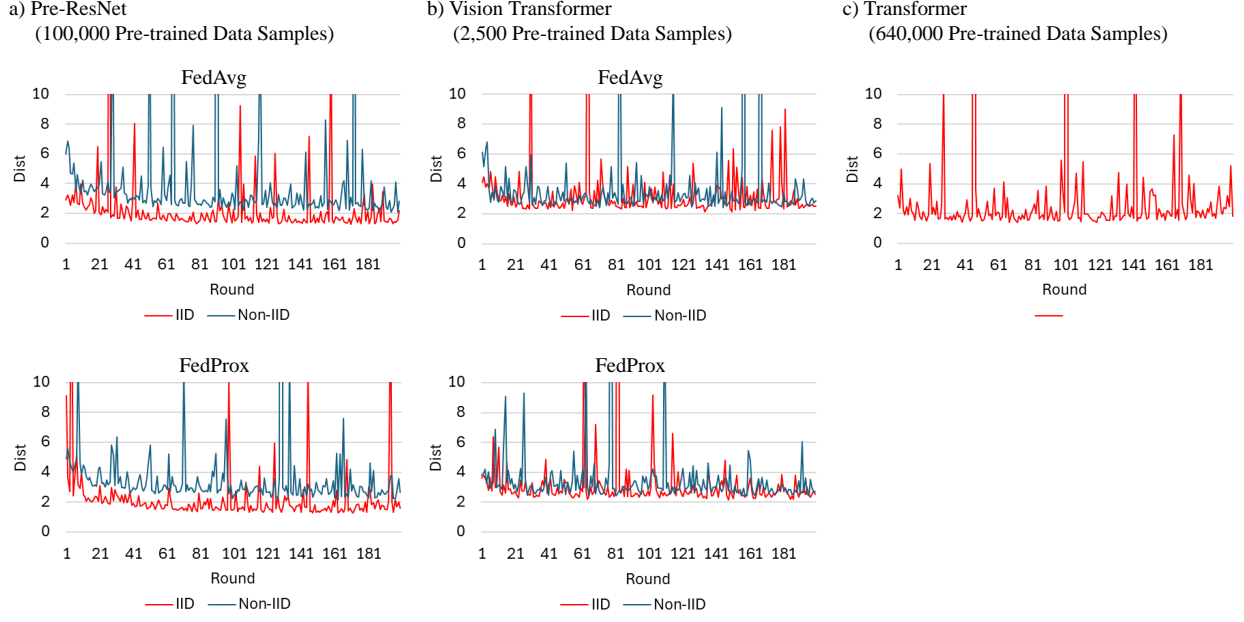


Figure 7: Distances (Dist) between the global model and the foundation model across aggregation rounds. The minimum Dist observed was 1.27, indicating significant differences in scale between the foundation model’s weights and the aggregated global model’s weights.

the weights of the aggregated global model. This means the foundation model’s weights differ in scale from the aggregated weights. To analyze the effect of distance intensity, we added Gaussian random noise based on the magnitude of each foundation model’s weights to the foundation model’s weights.

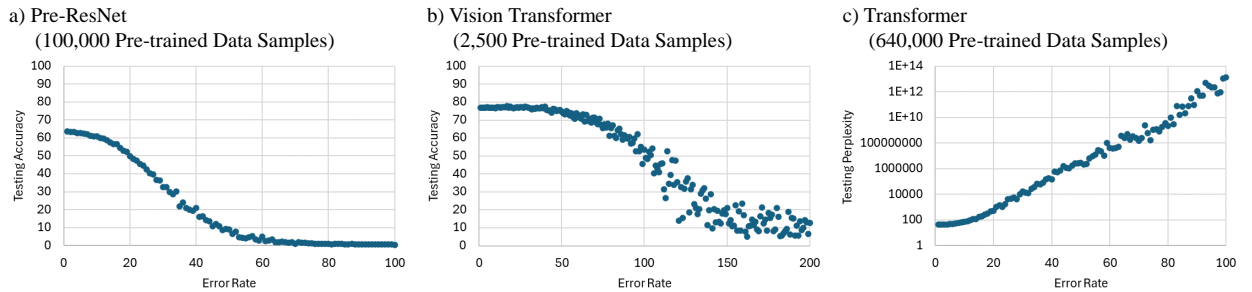


Figure 8: Testing accuracy according to the added noise. The x-axis error rate is calculated by the magnitude of the added Gaussian noise divided by the magnitude of the foundation model’s weights.

Figure 8 shows the testing accuracy as a function of the added noise. The x-axis represents the error rate, calculated by dividing the magnitude of the added Gaussian noise by the magnitude of the foundation model’s weights. We used the best-performing foundation models from those with

varying pre-trained sample sizes, as described in Section C. When a 127% error rate is applied, the Pre-ResNet model shows almost 0% testing accuracy, the Vision Transformer shows 30% testing accuracy, and the Transformer model exhibits excessively high testing perplexity. This empirical evidence indicates that extracting the foundation model’s knowledge is impossible after training begins from the global model. The diverse updates during training in FedBaF significantly disrupt the alignment between the foundation model’s weights and the global model, preventing any meaningful extraction of the foundation model’s information.

To this end, we examine the proximity of the global model, \mathbf{w}_t , to the foundation model and to the averaged local models, \mathbf{w}'_t , throughout the training process. We first determine the distances between \mathbf{w}'_t and \mathbf{w}_t and between \mathbf{w}_t and \mathbf{w}_{pre} :

$$\begin{aligned}\|\mathbf{w}_t - \mathbf{w}'_t\| &= \left\| \frac{1}{1 + \alpha\tau_t}(\mathbf{w}'_t + \alpha\tau_t\mathbf{w}_{pre}) - \mathbf{w}'_t \right\| \\ &= \frac{\alpha\tau_t}{1 + \alpha\tau_t} \|\mathbf{w}'_t - \mathbf{w}_{pre}\| \\ \|\mathbf{w}_t - \mathbf{w}_{pre}\| &= \left\| \frac{1}{1 + \alpha\tau_t}\mathbf{w}'_t + \alpha\tau_t\mathbf{w}_{pre} - \mathbf{w}_{pre} \right\| \\ &= \frac{1}{1 + \alpha\tau_t} \|\mathbf{w}'_t - \mathbf{w}_{pre}\|\end{aligned}$$

At the onset of training, both distances are equivalent since we make a strategic choice for the weight $\alpha_t\tau_0$ to be approximately 2. This simplifies the initial update rule for the global model such that the initial global model weights, \mathbf{w}_0 , are an unweighted average of the client’s updated model weights \mathbf{w}'_0 and the foundation model weights \mathbf{w}_{pre} . As the training progresses, $\alpha\tau_t$ typically decays to less than 1. We deduce for $t > 0$:

$$\frac{\alpha\tau_t}{1 + \alpha\tau_t} < \frac{1}{1 + \alpha\tau_t} \implies \|\mathbf{w}_t - \mathbf{w}'_t\| < \|\mathbf{w}_t - \mathbf{w}_{pre}\|$$

As $t \rightarrow \infty$, \mathbf{w}_t will drift away from \mathbf{w}_{pre} and towards \mathbf{w}'_t . Due to the intricate dissemination of learned insights across all model weights, and the complexities of high-dimensional weight spaces, it is difficult to reverse-engineer \mathbf{w}_{pre} from \mathbf{w}_t . Even a subset of weights does not provide enough information to predict the rest deterministically. The inherent complexity of the model weight (parameter) space is a natural defense mechanism in FedBaF.

G.2 Mitigating Backdoor Attacks

Backdoor attacks in FL involve embedding a dormant malicious function in a local model. Integrating foundation models mitigates such attacks by diluting the impact of individual client updates. Specifically, we have the updates

$$\Delta \mathbf{w}_{\text{client}}^t = \text{ClientUpdate}(\mathbf{w}_t)$$

$$\mathbf{w}_{t+1} = \frac{1}{1 + \alpha_t \tau_t} (\Delta \mathbf{w}_{\text{client}}^t + \alpha_t \tau_t \mathbf{w}_{\text{pre}})$$

Here, $\Delta \mathbf{w}_{\text{client}}^t$ is the update from client c at iteration t , and \mathbf{w}_{pre} is the foundation model weight. The factor τ_t controls the influence of the foundation model. This mathematical formulation showcases the security benefits of our method. By incorporating the foundation model, the aggregation counterbalances the (malicious) client update $\Delta \mathbf{w}_{\text{client}}^t$. This approach thus *enhances the system's resilience to adversarial attacks* by maintaining a consistent learning direction and reducing the impact of compromised updates.

G.3 Experiments on Variations of τ_t

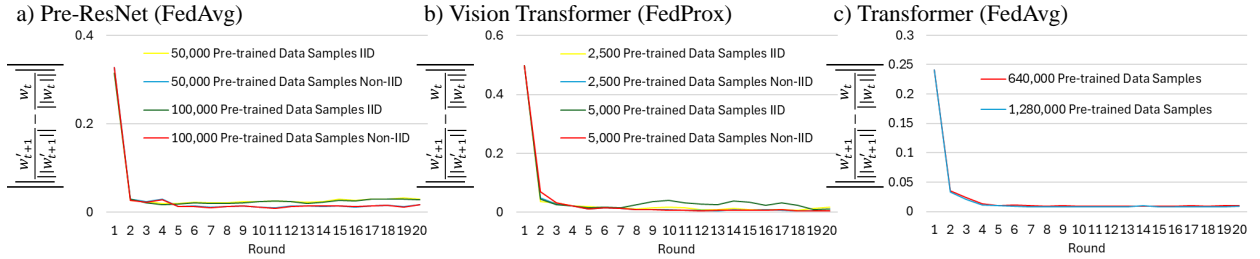


Figure 9: Variations of $\left\| \frac{\mathbf{w}'_{t+1}}{\mathbf{w}_{t+1}} \right\| - \left\| \frac{\mathbf{w}_t}{\mathbf{w}_t} \right\|$ ($= \tau_t \sqrt{t+1}$) across training rounds.

Figure 9 illustrates the non-adversarial IID and non-IID scenarios from Tables 3, 4, and 5. We observed that the numerator of τ_t (as referenced in Alg. 1 *Line 9*) consistently decreases towards 0, independent of the denominator ($\sqrt{t+1}$), after several rounds. This indicates that FedBaF benefits from the foundation model's guidance but retains the ability to effectively and quickly adapt to new data.